

Learning Deep Tree-based Retriever for Efficient Recommendation: Theory and Method

Ze Liu, Jin Zhang, Chao Feng, Defu Lian^{*}, Jie Wang, and Enhong Chen, *Fellow, IEEE*

Abstract—With the advancement of deep learning, deep recommendation models have achieved remarkable improvements in recommendation accuracy. However, due to the large number of candidate items in practice and the high cost of preference computation, these methods still suffer from low recommendation efficiency. The recently proposed tree-based deep recommendation models alleviate the problem by directly learning tree structure and representations under the guidance of recommendation objectives. To guarantee the effectiveness of beam search for recommendation accuracy, these models strive to ensure that the tree adheres to the max-heap assumption, where a parent node's preference should be the maximum among its children's preferences. However, they employ a one-versus-all strategy, framing the training task as a series of independent binary classification objectives for each node, which limits their ability to fully satisfy the max-heap assumption. To this end, we propose a Deep Tree-based Retriever (DTR for short) for efficient recommendation. DTR frames the training task as a softmax-based multi-class classification over tree nodes at the same level, enabling explicit horizontal competition and more discriminative top-k selection among them, which mimics the beam search behavior during training. To mitigate the suboptimality induced by the labeling of non-leaf nodes, we propose a rectification method for the loss function, which further aligns with the max-heap assumption in expectation. As the number of tree nodes grows exponentially with the levels, we employ sampled softmax to approximate optimization and thereby enhance efficiency. Furthermore, we propose a tree-based sampling method to reduce the bias inherent in sampled softmax. Theoretical results reveal DTR's generalization capability, and both the rectification method and tree-based sampling contribute to improved generalization. The experiments are conducted on four real-world datasets, validating the effectiveness of the proposed method.

Index Terms—Recommender System; Tree-based Index; Multi-class Classification; Sampled Softmax; Efficient Recommendation

1 INTRODUCTION

IN the information era, the overwhelming volume of daily information leads to significant information overload. The recommendation plays a crucial role in mitigating information overload by providing a personalized ranking list tailored to individual preferences. With the advancements of deep learning techniques, recommendation techniques also achieve remarkable improvements in ranking performance. The widespread application of these techniques has generated considerable economic benefits for various kinds of content providers in industrial companies.

Through the use of deep learning, we not only learn better representations for users, items, and contexts but also provide a more generalized expression for users' preference scores via neural networks than the widely-used inner product in matrix factorization. Both lead to stronger recom-

mandation performance, as demonstrated by models such as DIN [1], DIEN [2], NCF [3], CDL [4], and CKE [5]. However, the use of neural network-based preference functions brings online-serving challenges for recommender systems due to the high cost of preference computation. Generally speaking, immediate responses to adaptive recommendations are prerequisites for excellent customer experiences and custom retention. Existing popular and well-performed graph-based indexes (e.g., HNSW [6]), quantization-based indexes (e.g., PQ [7], AQ [8], and SCANN [9]), and hash-based indexes (e.g., SGDH [10]) are typically constructed based on inner product or Euclidean distance, making them unsuitable for accelerating the recommendations of deep models. In particular, neural network-based preference functions do not form a valid metric and are incompatible with Euclidean distance and inner product. As a result, two items that are close in Euclidean or inner-product space may have significantly different neural preference scores.

To guarantee the compatibility between search indexes with the neural network-based preference functions, it is a good solution to learn the search indexes together with the recommendation model under the guidance of recommendation objectives. The representative work is the tree-based deep model (i.e., TDM [11] and its improved version JTM [12]). These models use the balanced tree index, which is constructed by hierarchically clustering item representations from top to bottom. Given the tree, the top-k ranked items are retrieved through a layer-wise beam search, which selects the k largest tree nodes at each level based on neural preference scores from the top layer to the bottom layer.

Ze Liu and Chao Feng are with the School of Computer Science and Technology, University of Science and Technology of China, Hefei, Anhui 230027, China (e-mail: lz123@mail.ustc.edu.cn, chaofeng@mail.ustc.edu.cn)

Jin Zhang is with the School of Artificial Intelligence and Data Science, University of Science and Technology of China, Hefei, Anhui 230027, China (e-mail: jinzhang21@mail.ustc.edu.cn).

Defu Lian and Enhong Chen are with the State Key Laboratory of Cognitive Intelligence, School of Computer Science and Technology, School of Artificial Intelligence and Data Science, University of Science and Technology of China, Hefei, Anhui 230027, China (e-mail: liandefu@ustc.edu.cn, cheneh@ustc.edu.cn).

Jie Wang is with the Department of Electronic Engineering and Information Science, University of Science and Technology of China, Hefei, Anhui 230027, China (e-mail: jiewangx@ustc.edu.cn).

^{*}Corresponding author: Defu Lian (e-mail: liandefu@ustc.edu.cn).

This work has been submitted to the IEEE for possible publication. Copyright may be transferred without notice, after which this version may no longer be accessible.

In this way, beam search achieves logarithmic computation complexity w.r.t. the number of items. To guarantee the accuracy of beam search, these tree-based deep models rely on the following max-heap assumption: the preference scores of query for a parent node should be the maximum between the preference scores of its children node. For the sake of satisfying the assumption, these tree-based models cast the overall problem as a series of independent node-wise binary classification problems, treating nodes in the path from the root node to the leaf nodes corresponding to positive samples as positive and other randomly sampled nodes as negative. However, these tree-based models suffer from the following drawback: the max-heap assumption is not well satisfied by the used binary classification objectives due to the lack of explicit horizontal competition among the tree nodes at the same level. This drawback provides an opportunity to improve the accuracy of the efficient recommendation.

We propose a Deep Tree-based Retriever (DTR for short) for efficient recommendation. To satisfy the max-heap assumption as much as possible and mimic the beam search behavior in the training stage, DTR regards the training task as softmax-based multi-class classification over tree nodes at the same layer, which enables explicit horizontal competition and more discriminative top-k selection among them. Within this training mode, DTR utilizes a multi-class cross-entropy loss to optimize the deep model; however, theoretical analysis from the aspect of Bayes optimality indicates that this loss function still results in suboptimal performance under beam search induced by the labeling of non-leaf nodes, prompting us to propose a rectification method. Additionally, as the number of tree nodes increases exponentially with levels, the softmax loss becomes computationally expensive. Therefore, we resort to sampled softmax for approximation to promote training efficiency. We also develop a tree-based negative sampling method, guided by sampled softmax theory, to estimate the gradient of the original softmax loss more accurately. Moreover, we propose a tree learning method compatible with this training mode, enabling the alternating learning of the preference model and the tree index. Furthermore, we provide a generalization analysis of our proposed method, showing that it has good generalization capabilities and that the generalization could be enhanced through a negative sampling distribution closer to the softmax distribution and an increased number of branches in the tree structure.

As an extension of the preliminary paper [13], which contributed to the layer-wise softmax-based multi-class classification training mode and a tree learning method compatible with this training mode, we further make the following contributions:

- We identify the issue of suboptimality of multi-class classification training mode under beam search from the aspect of Bayes optimality and propose a rectification method to address this issue.
- We propose a tree-based negative sampling method for the multi-class classification problem in the tree. This sampling method can lead to more accurate estimations of loss gradient to reduce the inherent bias in sampled softmax.

- We provide a generalization analysis of the deep tree-based retriever, demonstrating the great generalization capability of our proposed methods.
- We evaluate the proposed methods on four real-world datasets and validate the superiority of DTR to the baselines and the effectiveness of the rectification method and the sampling method.

2 RELATED WORK

This study aims to enhance the accuracy of efficient recommendation through the deep tree-based retriever, focusing on both the methodologies and theoretical foundations. We begin by reviewing recent advancements in efficient recommendation. Subsequently, we survey recent efficient training techniques of recommendation and then delve into the theories closely connected to our study.

2.1 Efficient Recommendation

Efficient recommendation relies on building a search index, including LSH [14], inverted index [15, 16], tree index [17, 18] and graph index [6] for all items. The recommender system usually uses the inner product for computing preference scores, and the top-k recommendation can be cast into the maximum inner product search (MIPS) problem. The search index is usually constructed based on Euclidean distance and has been extended to the inner product. This extension can be achieved by establishing the relationship between nearest neighbor search and MIPS [19, 20, 21], or learning from either item representations [22, 23, 24, 25] or the raw data directly [26, 27, 28, 29]. With the introduction of deep learning into the recommender systems, the preference score function becomes complicated, such that it is challenging to transform from neural ranking to NNS or MIPS. Existing work either directly used metric-based index[30], or learns search index from raw data directly together with recommendation models [11, 12, 31].

2.2 Efficient Training Techniques of Recommendation

2.2.1 Negative Sampling in RecSys

Negative sampling is an important method to address the negative missing and exposure bias problems and to speed up the convergence of recommender training [32, 33, 34]. It includes static sampling, such as uniform sampling [35], popularity sampling, and adaptive sampling. The adaptive sampling is context-dependent, whose representation work includes adaptive oversampling [35], rejection sampling [36, 37], clustering-based sampling [32], and dynamic negative sampling [38]. The core idea of these adaptive samplers is that items with larger preference scores should be sampled with higher probability.

2.2.2 Techniques of Speeding Up Softmax Computation

In natural language applications, it is very computationally expensive to represent an output distribution over the choice of a word based on the softmax function. To enhance computational efficiency, many approximate algorithms are proposed. For example, hierarchical softmax [39] and lightRNN [40] decompose the probabilities, and Contrastive Divergence [41] approximates the gradient based

on MCMC. As an alternative, negative sampling is also widely used to reduce the computational cost of training the models. The representative work includes Noise-Contrastive Estimation [42] with the unigram distribution as a sampler, Generative Adversarial Networks [43, 44] with a neural-network empowered sampler, Self-Contrast Estimator [45] by the model in the immediately preceding epoch as a sampler, self-adversarial negative sampling [46] and Kernel-based sampling [47] with the tree index.

2.3 Theoretical Work

2.3.1 Bayes Optimality in Multi-class Classification and Hierarchical Classification

Bayes optimality aims for the learned classifier to achieve the highest possible performance on previously unseen data distributions. In the realm of multi-class classification, Bayes optimality has been extensively studied [48, 49]. Top- k Bayes optimality is introduced to address ambiguities in ground truth classes by focusing on the k most likely predicted classes [50, 51, 52]. In recent years, researchers have begun to extend Bayes optimality to hierarchical classification. [53] utilizes it to measure the performance of probability estimation using tree models in hierarchical classification. [54] examines performance degradation of tree models under beam search in hierarchical classification and proposes a method for achieving Bayes optimality under beam search.

2.3.2 Generalization Bounds for Multi-class Classification

Generalization error bounds are used to provide guarantees for the generalization ability of the learned classifier. [55] provides data-dependent generalization bounds for multi-class classification based on margins. [56] further develop these bounds with multiple kernels. To accommodate the scenario with a large number of classes, data-dependent generalization error bounds with a mild dependency on the number of classes have also been studied [57]. The aforementioned bounds primarily focus on flat structures. In the context of hierarchical structures, [58] proposes a multi-class, hierarchical data-dependent generalization error bound for kernel classifiers in large-scale taxonomies.

3 PRELIMINARIES

3.1 Problem Definition and Notation

Consider a user space \mathcal{U} and an item set \mathcal{Y} , where each user in \mathcal{U} is characterized by its historical interaction sequence and other available profiles. Assume that the data is generated i.i.d. from some distribution \mathbb{P} over $\mathcal{U} \times \mathcal{Y}$, and an instance is represented as $(u, y) \in \mathcal{U} \times \mathcal{Y}$, with the corresponding joint probability $p(u, y)$. For a given user u , the conditional probability of observing item y is denoted by $\eta_y(u) = p(y|u)$. Given the user u , the objective of the recommendation is to return the top- k items with the highest conditional probabilities $\eta_y(u)$.

In this paper, we use the following notational conventions: bold lowercase and uppercase letters for vectors and matrices respectively, such as \mathbf{a} and \mathbf{A} , and non-bold letters for scalars or constants, such as k and C . For vector \mathbf{a} , a_i denotes its i -th component and $\|\mathbf{a}\|_p$ denotes the ℓ_p norm.

For matrix, $\|\mathbf{A}\|_p = \sup_{\|\mathbf{x}\|_p=1} \|\mathbf{Ax}\|_p$ denotes matrix norms induced by vector p -norms. We denote the set $\{1, 2, \dots, m\}$ by $[m]$ for any natural number m . Other notations will be explicitly defined in the corresponding section. Additionally, we summarize some important and commonly used notations of this paper in Appendix A.

3.2 Tree Models

Modern recommender systems need to retrieve top- k items from a large-scale corpus (i.e., $|\mathcal{Y}|$ ranges from millions to billions or even tens of billions). To tackle the top- k retrieval for such a large corpus efficiently and effectively, TDM [11] and JTM [12] propose the tree-based recommendation models, which consists of a max-heap-like tree index and an advanced neural preference model. In this subsection, we will introduce the tree index and the preference model, detail the top- k retrieval process, and subsequently elaborate on the tree model's training process in TDM and JTM.

3.2.1 Tree Index

The B -ary tree \mathcal{T} is used to form the tree index, which consists of a set of nodes \mathcal{N} , where the nodes at the j -th level are denoted by \mathcal{N}^j . The entire node set $\mathcal{N} = \bigcup_{j=0}^H \mathcal{N}^j$, with the tree height $H = \lceil \log_B |\mathcal{Y}| \rceil$ to accommodate all items. The bijective mapping $\pi : \mathcal{N}^H \rightarrow \mathcal{Y}$ maps each leaf node to a unique item, with the inverse mapping denoted by $\pi^{-1} : \mathcal{Y} \rightarrow \mathcal{N}^H$. Accordingly, an item y is mapped to a leaf and corresponds to a path in the tree from the root to that leaf.

For each level j , we denote the number of nodes in that level as $N_j = |\mathcal{N}^j|$ and assume the nodes are listed in a fixed order, denoted as $(n_1^j, n_2^j, \dots, n_{N_j}^j)$. For the i -th node in the j -th level, denoted as n_i^j , let $\rho^l(n_i^j) \in \mathcal{N}^l$ represent its ancestor in level l ($0 \leq l \leq j$), where $\rho^j(n_i^j)$ refers to the node itself. The set $\mathcal{C}(n_i^j) \subseteq \mathcal{N}$ represents child nodes of n_i^j , while $\mathcal{L}(n_i^j) \subseteq \mathcal{N}^H$ denotes the leaf nodes within the subtree rooted at n_i^j . The function δ is introduced to return the index of a node within its level, i.e., $\delta(n_i^j) = i$. The j -th ancestor in item y 's corresponding path is $\rho^j(\pi^{-1}(y))$ and its index in this level is denoted as $\delta^j(y) = \delta(\rho^j(\pi^{-1}(y)))$.

3.2.2 Preference Model

The retrieval process is guided by users' preferences for tree nodes. As the real preference of user u for node n is unavailable, a preference model $\mathcal{M} : \mathcal{U} \times \mathcal{N} \rightarrow \mathbb{R}$ predicts the preference scores. A variation of DIN [1] is commonly used as the preference model in tree-based models. In this subsection, we provide a detailed description of DIN.

In the DIN model, the historical interaction sequence of a user u serves as the input. Specifically, the model takes as input a matrix of item embedding vectors, denoted as $\mathbf{A}^{(u)}$:

$$\mathbf{A}^{(u)} = \left[\mathbf{a}_1^{(u)}, \mathbf{a}_2^{(u)}, \dots, \mathbf{a}_K^{(u)} \right] \in \mathbb{R}^{d \times K}, \quad (1)$$

where the last K items of u 's historical interaction sequence are considered, and $\mathbf{a}_k^{(u)}$ represents the embedding of k -th item. The model employs a two-layer fully connected

network to compute the weight between the node n and the k -th interacted item, which can be expressed as:

$$w_k^{(u)}(n) = \phi \left(\mathbf{W}_w^{(2)} \phi \left(\mathbf{W}_w^{(1)} \left[\mathbf{a}_k^{(u)}; \mathbf{a}_k^{(u)} \odot \mathbf{w}_n; \mathbf{w}_n \right] \right) \right) \in \mathbb{R}, \quad (2)$$

where $\mathbf{W}_w^{(1)} \in \mathbb{R}^{h \times 3d}$, $\mathbf{W}_w^{(2)} \in \mathbb{R}^{1 \times h}$, \mathbf{w}_n is the embedding of the node n , and ϕ is the activation function, which is PReLU in the practical model setting. In the following, we omit n and use the notation $w_k^{(u)}$ to denote the weight.

To enable a dynamic representation of user interests, the historical interaction sequence is partitioned into K' time windows, where the t -th time window T_t of length k is a set of continuous indices, i.e., $T_t = \{i_0 + 1, \dots, i_0 + k\}$. These time windows are mutually exclusive, and their union is exactly $[K']$. In the t -th time window, the interacted item embeddings are aggregated using weights calculated in Eq. (2), as shown below:

$$\mathbf{z}_t^{(u)} = \sum_{k \in T_t} w_k^{(u)} \mathbf{a}_k^{(u)} \in \mathbb{R}^d. \quad (3)$$

Then, the concatenation of K' aggregated embeddings and the embedding of node n will be fed into an MLP with L hidden layers to output the user's preference score for node n_i^j , which can be expressed as follows:

$$f_{\text{DIN}}(u, n) = \mathbf{W}_L \cdot \phi_{L-1} \circ \dots \circ \phi_1 \left([\mathbf{z}_1^{(u)}; \mathbf{z}_2^{(u)}; \dots; \mathbf{z}_{K'}^{(u)}; \mathbf{w}_n] \right) \quad (4)$$

where $\mathbf{W}_L \in \mathbb{R}^{1 \times d_{L-1}}$, and the function $\phi_k(\mathbf{x})$ is defined:

$$\phi_k(\mathbf{x}) = \phi(\mathbf{W}_k \mathbf{x}) \in \mathbb{R}^{d_k \times 1}, \forall k \in [L-1]. \quad (5)$$

The element-wise activation function ϕ is Lipschitz continuous with a Lipschitz constant c_ϕ , has the property $\sigma(0) = 0$ and $\mathbf{W}_k \in \mathbb{R}^{d_k \times d_{k-1}}$ represents the weight matrix.

The preference model \mathcal{M} is exactly the function space of f_{DIN} . Given a user u , the preference score for the node n_i^j is denoted as $o_i^j(u) = f_{\text{DIN}}(u, n_i^j)$. For simplicity, the user u is omitted, and the notation o_i^j is adopted for the remainder of this paper.

3.2.3 Top- k Retrieval Process

As each item is mapped to a leaf, the top- k retrieval in recommendation is transformed into retrieving the k leaf nodes with the highest preference scores for a given user u . If u 's preference for any tree node is available, we can retrieve the top- k leaf nodes by only searching the top- k nodes at each level, from the top to the bottom of the tree. In cases where the tree is precisely structured as a max-heap, this process guarantees the correct top- k leaf nodes are retrieved finally. Moreover, the time complexity of this process is logarithmic w.r.t. the number of items, as a constant number of nodes are searched at each layer, and the number of layers scales logarithmically with the number of items.

The above retrieval process is presented in Algorithm 1, where $p^{\mathcal{M}}(n|u)$ is the user u 's preference for node n computed by the preference model \mathcal{M} . Essentially, this process is a layer-wise beam search with beam size k along the tree \mathcal{T} , guided by the preference o_i^j between the user u and the node n_i^j , and can be formulated as follows:

$$\mathcal{B}^j(u) \in \arg \text{Topk } o_i^j, \quad i \in \tilde{\mathcal{B}}^j(u) \quad (6)$$

Algorithm 1: BEAM SEARCH: LAYER-WISE RETRIEVAL

Input: User u , tree \mathcal{T} , beam size k , the preference model \mathcal{M}

Output: top- k items

- 1: Result set $A = \emptyset$, candidate set $Q = \{\text{root node } n_1^0\}$;
- 2: **while** Q is not empty **do**
- 3: Remove all leaf nodes from Q and add them into result set A if Q contains leaf nodes;
- 4: Compute preference $p^{\mathcal{M}}(n|u)$ through \mathcal{M} for each node in set Q ;
- 5: Parents = {top- k nodes of Q according to $p^{\mathcal{M}}(n|u)$ };
- 6: $Q = \{\text{children of node } n \mid n \in \text{Parents}\}$;
- 7: **end while**
- 8: **return** The top- k items w.r.t. the top- k leaf nodes according to $p^{\mathcal{M}}(n|u)$, $n \in A$.

where $\mathcal{B}^j(u)$ denotes the set of indices of selected nodes in the j -th level for the user u , and $\tilde{\mathcal{B}}^j(u) = \{\delta(n) \mid n \in \bigcup_{i \in \mathcal{B}^{j-1}(u)} \mathcal{C}(n_i^{j-1})\}$ represents the index set of nodes to be expanded in the j -th level. It's important to note that Eq. (6) employs the symbol “ \in ” instead of “ $=$ ” because ties in probabilities may occur, leading to multiple potential sets of top- k nodes. If $|\tilde{\mathcal{B}}^j(u)| < k$, then all nodes in j -th level will be selected. By recursively applying Eq. (6) until the H -th level, the top- k leaf nodes $\mathcal{B}^H(u)$ are retrieved, and the final retrieved item set for the user u is

$$\hat{\mathcal{Y}}(u) = \{\pi(n_i^H) \mid i \in \mathcal{B}^H(u)\}. \quad (7)$$

3.2.4 Training Process in TDM and JTM

Both TDM and JTM alternatively learn the preference model and the tree to enhance the tree model. To learn the preference model, TDM and JTM regard the training task as a series of independent node-wise binary classification problems. Supposing user u has an interaction with an item that corresponds to a leaf node, this leaf node and its ancestors are positive nodes with label 1, while all other nodes in the tree are negative nodes with label 0. Then, the training loss for user u is

$$\begin{aligned} \mathcal{L}(u, S_u^+, S_u^-) = & - \sum_{n \in S_u^+} z_u(n) \log p(\hat{z}_u(n) = 1|u) \\ & - \sum_{n \in S_u^-} (1 - z_u(n)) \log p(\hat{z}_u(n) = 0|u). \end{aligned} \quad (8)$$

S_u^+ and S_u^- denote the positive node set and negative node set for user u , respectively. $z_u(n)$ denotes the label of node n for user u . $p(\hat{z}_u(n) = 1|u)$ and $p(\hat{z}_u(n) = 0|u)$ denote the like and dislike probabilities for user u to node n , which are exactly corresponding to the two outputs of preference model. Since using all negative nodes to train the model is unacceptable both in time-consuming and memory consumption, both TDM and JTM sample a set of negative nodes (denoted as $S_u'^-$) uniformly from all the negative nodes. Then $\mathcal{L}(u, S_u^+, S_u'^-)$ is used as training loss.

To learn the tree, both TDM and JTM adopt a hierarchical clustering-like method. TDM clusters all the items recursively by k-means using the item embedding until

each cluster only contains one item. The recursive clustering process can form a tree structure, and the item in each final cluster is exactly mapped to a leaf node. JTM assigns all the items to each node from the top layer to the bottom layer so that the sum of the log-likelihoods for all users on each layer can be maximized. Interested readers can refer to TDM [11] and JTM [12] for more details about how to learn the trees respectively. In our work, we propose a new tree learning method compatible with our proposed preference model learning mode.

4 LEARNING DEEP TREE-BASED RETRIEVER

The performance of the deep tree-based retriever depends on both the preference model and the tree index. To learn the deep tree-based retriever, we need to optimize the preference model (i.e., the deep model that outputs the scores between users and nodes) and update the tree index (i.e., the mapping π between items and leaf nodes). Since the tree index updating is discrete and non-differentiable, we learn the preference model and the tree index alternately. Concretely, we fix the mapping π and apply stochastic gradient descent to optimize the preference model; then, we fix the preference model and use a discrete optimization method to update the mapping π . This alternating process of model optimization and tree index updating improves retrieval performance gradually until convergence.

In this section, we elaborate on the optimization of the preference model and the updating of the tree index. Subsection 4.1 and Subsection 4.2 present our training mode and rectification method for model optimization. Subsection 4.3 introduces the negative sampling method in practical optimization. Finally, Subsection 4.4 describes the process for updating the tree index.

4.1 Softmax-based Multi-class Classification Training Mode

To address the shortcomings of the training mode in TDM and JTM, we develop a layer-wise training mode in this section. We regard the training task as a multi-class classification problem at each layer, employing the classic multi-class cross-entropy loss to optimize the preference model. Upon examining the Bayes optimality of this training scheme, we observe that the traditional multi-class cross-entropy loss leads to suboptimality under beam search.

4.1.1 Multi-class Cross-entropy Loss

TDM and JTM regard the training task as a series of independent node-wise binary classification problems, and binary cross-entropy loss is utilized as the training loss. In this way, each node contributes to the training loss individually, resulting in a lack of explicit horizontal competition among nodes within the same layer. However, layer-wise retrieval is conducted from the top layer to the bottom layer, requiring a comparison of each candidate in the same layer with every other candidate. There is a gap between training and prediction in TDM and JTM. To address the above issue, we propose a layer-wise training mode that regards the training task as a multi-class classification problem.

In the context of this training mode, at layer j , which consists of N_j nodes, each node corresponds to a class, and

multi-class classification with N_j classes is performed at that layer. Given an instance (u, y) , we attach a label $z_i^j(u, y)$ to each node n_i^j to indicate whether the node is positive or negative. For simplicity, we will omit u, y and use the notation z_i^j in the rest of the paper. The positive node can be identified by backtracking from the item y 's mapping leaf node to the root node, as demonstrated in TMD and JTM, and the corresponding label will be assigned as 1, i.e., $z_{\delta^j(y)}^j = 1$. The remaining $N_j - 1$ nodes are the negative nodes with the label 0. The preference model outputs a score for each node, resulting in N_j preference scores for the j -th layer, which is tailored for the multi-class classification task with N_j classes. For the given instance (u, y) , the index of the positive node in layer j is $\delta^j(y)$. Then, the training loss at layer j , specifically the multi-class cross-entropy loss, is calculated as follows:

$$\mathcal{L}_j(u, y) = -\log p_{\delta^j(y)}^j = -\log \frac{\exp o_{\delta^j(y)}^j}{\sum_{k=1}^{N_j} \exp o_k^j}. \quad (9)$$

From Eq. (9), we can know that all the nodes of layer j contribute to the training loss simultaneously, which relieves the gap between training and prediction. The training loss w.r.t. the whole tree is the sum of the losses for each layer.

4.1.2 Suboptimality of Multi-class Cross-entropy Loss Under Beam Search

Treating the training task as a multi-class classification problem at each layer can alleviate shortcomings associated with binary classification. However, the multi-class cross-entropy loss still leads to suboptimality under beam search induced by the labeling of non-leaf nodes. In this subsection, we demonstrate how multi-class cross-entropy loss results in suboptimal outcomes under beam search.

Similar to Bayes optimality defined in [52, 54], we define the top- k retrieval Bayes optimality under beam search to adapt to our hierarchical multi-class classification setting:

Definition 1 (Top- k Retrieval Bayes Optimal). *Given the beam size k , the tree model consist of a tree \mathcal{T} and a preference model \mathcal{M} is top- k retrieval Bayes optimal, if the following equation*

$$\hat{\mathcal{Y}}(u) \in \arg \operatorname{Topk}_{y \in \mathcal{Y}} \eta_y(u) \quad (10)$$

holds for any $u \in \mathcal{U}$.

The underlying idea of Definition 1 is straightforward: for each user u , a top- k retrieval Bayes optimal tree model should return the k items with the highest conditional probabilities.

Building on the Definition 1, we show that optimizing a tree model using multi-class cross-entropy loss can result in suboptimal outcomes under beam search. Our demonstration leverages the property of Bregman divergence [59]. Let N denote the number of classes. For a strictly convex and differentiable function $\psi : \mathbb{R}^N \rightarrow \mathbb{R}$, the Bregman divergence $D_\psi : \mathbb{R}^N \times \mathbb{R}^N \rightarrow \mathbb{R}$ induced by ψ is defined as follows:

$$D_\psi(\mathbf{z}, \mathbf{o}) = \psi(\mathbf{z}) - \psi(\mathbf{o}) - \nabla \psi(\mathbf{o})^T (\mathbf{z} - \mathbf{o}), \quad (11)$$

where $\mathbf{z}, \mathbf{o} \in \mathbb{R}^N$. Previous work [52, 59] has demonstrated the rank property of optimizing the loss functions that

can be expressed as Bregman divergence. We present their theoretical result in the following. We first introduce the definition of rank consistent as follows:

Definition 2 (Rank Consistent). *Given $\mathbf{x}, \mathbf{y} \in \mathbb{R}^N$, we say that \mathbf{x} is rank consistent w.r.t. \mathbf{y} , denoted as $R(\mathbf{x}, \mathbf{y})$, if and only if for all $i, j \in [N]$,*

$$x_i > x_j \iff y_i > y_j.$$

Then, we state their theorem with modifications to adapt to our problem setting:

Theorem 1 (Theorem 3.1 of [52]). *Given a convex, differentiable function $\psi : \mathbb{R}^N \mapsto \mathbb{R}$. Let \mathbf{z} be a random vector taking values in \mathbb{R}^N for which both $\mathbb{E}[\mathbf{z}]$ and $\mathbb{E}[\psi(\mathbf{z})]$ are finite. If continuous function $g : \mathbb{R}^N \mapsto \mathbb{R}^N$ satisfies that $R(\mathbf{s}, g(\mathbf{s}))$ holds for $\forall \mathbf{s} \in \text{domain}(g)$, and $\mathbb{E}[\mathbf{z}] \subseteq \text{range}(g)$, then*

$$\underset{\mathbf{s} \in \mathbb{R}^N}{\text{argmin}} \mathbb{E}_{\mathbf{z}} [D_{\psi}(\mathbf{z}, g(\mathbf{s})] \subseteq \left\{ \mathbf{s} \in \mathbb{R}^N \mid R(\mathbf{s}, \mathbb{E}_{\mathbf{z}}[\mathbf{z}]) \right\}.$$

As previously mentioned, a label z_i^j is attached to the node n_i^j for a given instance (u, y) . When the user u is fixed, z_i^j is a conditional random variable, with its randomness depending on the item y . The variables in the j -th layer compose the random vector \mathbf{z}^j . As the label $z_{\delta^j(y)}^j$ is set to 1 and other labels in the j -th layer are set to 0 for the instance (u, y) , the expectation of \mathbf{z}^j for a given user u is as follows:

$$\mathbb{E}[\mathbf{z}^j|u] = \left(\sum_{n \in \mathcal{L}(n_1^j)} \eta_{\pi(n)}, \sum_{n \in \mathcal{L}(n_2^j)} \eta_{\pi(n)}, \dots, \sum_{n \in \mathcal{L}(n_{N_j}^j)} \eta_{\pi(n)} \right). \quad (12)$$

For simplicity, we omit u and use notation $\eta_{\pi(n)}$ to represent $\pi(n)$'s conditional probability given the user u .

The multi-class cross-entropy loss (i.e., Eq. (9)) is actually a Bregman divergence. By taking $\psi(s) = \sum_{n=1}^N s_n \log s_n$ and $g(\mathbf{o})_n = \exp o_n / \sum_{k=1}^N \exp o_k$, the multi-class cross-entropy loss

$$\mathcal{L}(\mathbf{e}^{(i)}, \mathbf{o}) = -\log \frac{\exp o_i}{\sum_{n=1}^N \exp o_n} \quad (13)$$

can be expressed as Bregman divergence:

$$\mathcal{L}(\mathbf{e}^{(i)}, \mathbf{o}) = D_{\psi}(\mathbf{e}^{(i)}, g(\mathbf{o})). \quad (14)$$

Here, $\mathbf{o}, \mathbf{e}^{(i)} \in \mathbb{R}^N$, and $\mathbf{e}^{(i)}$ is a one-hot vector where the i -th component is 1 and other components are 0.

With the fact that multi-class cross-entropy loss is a Bregman divergence and the softmax function g satisfies $R(\mathbf{s}, g(\mathbf{s}))$ for any $\mathbf{s} \in \mathbb{R}^N$, according to Theorem 1, when given user u , minimizing the conditional risk of multi-class cross-entropy loss of layer j , i.e.,

$$\mathcal{R}_j(u) = \mathbb{E}_{y \sim \eta_y(u)} [\mathcal{L}_j(u, y)] = \mathbb{E}_{y \sim \eta_y(u)} \left[-\log \frac{\exp o_{\delta^j(y)}^j}{\sum_{k=1}^{N_j} \exp o_k^j} \right], \quad (15)$$

aligns the ranks of each component in \mathbf{o}^j with those in $\mathbb{E}[\mathbf{z}^j|u]$ (i.e., $R(\mathbf{o}^j, \mathbb{E}[\mathbf{z}^j|u])$), where \mathbf{o}^j is the preference score vector for the j -th layer whose i -th component is o_i^j . Since the multi-class cross-entropy loss is optimized for each layer (i.e., Eq. (9)), $R(\mathbf{o}^j, \mathbb{E}[\mathbf{z}^j|u])$ holds for $1 \leq j \leq H$.

Therefore, we can identify that it is suboptimal under beam search.

Proposition 1. *The multi-class cross-entropy loss results in the tree model not being top- k retrieval Bayes optimal.*

Proof. We complete the proof by giving a non-optimal example. Considering the item set \mathcal{Y} with $|\mathcal{Y}| = 8$, we directly map i -th item to i -th leaf node, and construct the corresponding binary tree with height $H = 3$. Given the user u_0 , the conditional probability vector is $\eta(u_0) = (0.21, 0, 0.12, 0.18, 0.19, 0, 0.16, 0.14)$, where the i -th component is the conditional probability of i -th item. According to Eq. (12), the expectation vector is $(0.21, 0.3, 0.19, 0.3)$ and $(0.51, 0.49)$ for 2nd layer and 1st layer, respectively.

Let beam size $k = 3$. Since optimizing the multi-class cross-entropy loss leads to $R(\mathbf{o}^j, \mathbb{E}[\mathbf{z}^j|u])$ for $1 \leq j \leq H$, when performing the beam search along the tree, the result of $\text{argTopk } \mathbf{o}_i^j$ is identical to the result of $\text{argTopk } \mathbb{E}[z_i^j|u]$.

The expanded nodes in 2nd layer are $\{1^{(2)}, 2^{(2)}, 4^{(2)}\}$, and in 3rd layer are $\{1^{(3)}, 4^{(3)}, 7^{(3)}\}$, which is the final retrieved result. However, the optimal result is $\{1^{(3)}, 4^{(3)}, 5^{(3)}\}$ under beam search with beam size $k = 3$. \square

4.2 Rectification Under Beam Search

In this subsection, we introduce how to mitigate the issue of suboptimality under beam search, which is achieved by modifying the original label assignment for the non-leaf nodes and the loss function. Besides, we provide the theoretical support for these modifications and propose effective solutions for their practical implementation.

4.2.1 Label Rectification

For an observed instance (u, y) , do not directly assign labels of the ancestors of the leaf node $\pi^{-1}(y)$ to 1. Only if the item y has the largest conditional probability among the items in $\pi(\mathcal{L}(n_i^j))$, can the label z_i^j be assigned as 1. We slightly abuse notation by using $\pi(\mathcal{L}(n_i^j))$ to denote the set of items mapped from the leaf nodes in $\mathcal{L}(n_i^j)$. Denote the rectified label by \bar{z}_i^j , the formalization of assignment is as follows:

$$\bar{z}_i^j = \begin{cases} 1, & n_i^j = \rho^j(\pi^{-1}(y)) \wedge y = \underset{y' \in \pi(\mathcal{L}(n_i^j))}{\text{argmax}} \eta_{y'} \\ 0, & \text{else.} \end{cases}$$

With such a rectified assignment of the label of nodes, given the user u , for each node n_i^j , we can calculate the expectation of the corresponding random variable:

$$\mathbb{E}_{y \sim \eta_y(u)} [\bar{z}_i^j|u] = \sum_{y \in \mathcal{Y}} \bar{z}_i^j * \eta_y(u) = \max_{n \in \mathcal{L}(n_i^j)} \eta_{\pi(n)},$$

so the expectation of j -th layer's random vector is

$$\mathbb{E}[\bar{\mathbf{z}}^j|u] = \left(\max_{n \in \mathcal{L}(n_1^j)} \eta_{\pi(n)}, \max_{n \in \mathcal{L}(n_2^j)} \eta_{\pi(n)}, \dots, \max_{n \in \mathcal{L}(n_{N_j}^j)} \eta_{\pi(n)} \right), \quad (16)$$

indicating the rectified labels can align the tree with the max-heap in expectation.

Since we regard the recommendation task as a multi-class classification problem, the conditional probabilities

for a given user u satisfy the normalization condition $\sum_{y \in \mathcal{Y}} \eta_y(u) = 1$. The current expectations of each layer's random variables corresponding to the rectified label \bar{z}_i^j are not normalized; hence, a normalization term $\alpha^j(u) = \sum_{i=1}^{N_j} \bar{z}_i^j(u)$ should be applied to the unnormalized rectified label, resulting in the following label assignment:

Definition 3 (Label Rectification). *For a given instance (u, y) , the normalized rectified label \tilde{z}_i^j of node n_i^j is defined as follows:*

$$\tilde{z}_i^j = \begin{cases} \frac{1}{\alpha^j(u)}, & n_i^j = \rho^j(\pi^{-1}(y)) \wedge y = \operatorname{argmax}_{y' \in \pi(\mathcal{L}(n_i^j))} \eta_{y'} \\ 0, & \text{else.} \end{cases} \quad (17)$$

4.2.2 The Induced Loss Function

Under the above label rectification method, instead of converting each layer's labels into a one-hot vector, the default value of 1 is replaced with a positive real number. To adapt to the label rectification method and utilize the property of Bregman divergence again, the following loss function is proposed:

$$\tilde{\mathcal{L}}(\mathbf{e}^{(i)}(w), \mathbf{o}) = -w \log \left(\frac{\exp o_i}{\sum_{k=1}^N \exp o_k} \right) + w \log w + w - 1. \quad (18)$$

Here, $w \in [0, +\infty)$, $\mathbf{e}^{(i)}(w), \mathbf{o} \in \mathbb{R}^N$, and $\mathbf{e}^{(i)}(w) = (0, \dots, 0, w, 0, \dots, 0)$ where the i -th component is w , which will be set to \tilde{z}_i^j as presented in Eq. (17) to adapt to the label rectification method, and other components are 0.

Compared to the original multi-class cross-entropy loss (i.e., Eq. (9)), the loss function in Eq. (18) includes a slight modification by incorporating a weighting factor and a constant addition for a given w , which is fully compatible with the rectified label. Importantly, it retains its nature as a Bregman divergence, allowing for theoretical analysis based on Theorem 1.

Proposition 2. *The loss function in Eq. (18) can be expressed as Bregman divergence.*

Proof. See Appendix B.1. \square

4.2.3 Theoretical Support

With the above label rectification method and the induced loss function, for a given instance (u, y) , the following loss is optimized in the j -th layer:

$$\tilde{\mathcal{L}}_j(u, y) = \tilde{\mathcal{L}}(\mathbf{e}^{(\delta^j(y))}(\tilde{z}_{\delta^j(y)}^j), \mathbf{o}^j).$$

As indicated in Proposition 2, $\tilde{\mathcal{L}}$ still owns the property of Bregman divergence. Notice with the normalization, $\mathbb{E}[\tilde{z}^j|u] \subseteq \text{range}(g)$ holds for $1 \leq j \leq H$. Then, for any user $u \in \mathcal{U}$, by the Theorem 1, we have

$$\operatorname{argmin}_{\mathbf{o}^j \in \mathbb{R}^{N_j}} \tilde{\mathcal{R}}_j(u) \subseteq \left\{ \mathbf{o}^j \in \mathbb{R}^{N_j} \mid R(\mathbf{o}^j, \mathbb{E}[\tilde{z}^j|u]) \right\},$$

where $\tilde{\mathcal{R}}_j(u) = \mathbb{E}_{y \sim \eta_y(u)} [\tilde{\mathcal{L}}_j(u, y)]$ is the conditional risk for user u of j -th layer. This indicates that optimizing the modified loss with rectified labels can lead the tree model to be top- k retrieval Bayes optimal under beam search. Specifically, we have the following theoretical results:

Lemma 1. *Given a user $u \in \mathcal{U}$, if the tree model, which consists of a tree \mathcal{T} and a preference model \mathcal{M} , satisfies $R(\mathbf{o}^j, \mathbb{E}[\tilde{z}^j|u])$ for all $1 \leq j \leq H$, then*

$$\mathcal{B}^j(u) \in \operatorname{argTopk}_{i \in [N_j]} \mathbb{E}[\tilde{z}_i^j|u] \implies \mathcal{B}^{j+1}(u) \in \operatorname{argTopk}_{i \in [N_{j+1}]} \mathbb{E}[\tilde{z}_i^{j+1}|u]$$

holds for any beam size k within the range $1 \leq j \leq H - 1$.

Proposition 3. *For any user $u \in \mathcal{U}$, if the tree model, which consists of a tree \mathcal{T} and a preference model \mathcal{M} , satisfies that $R(\mathbf{o}^j, \mathbb{E}[\tilde{z}^j|u])$ for all $1 \leq j \leq H$, then the tree model is top- k retrieval Bayes optimal for any beam size k .*

The proofs of Lemma 1 and Proposition 3 are provided in Appendix B.2 and B.3, respectively. The above theoretical analysis demonstrates that optimizing the modified loss function with the normalized rectified label can mitigate the issue of suboptimality under beam search of original multi-class cross-entropy loss.

4.2.4 Practical Implementation

The above analysis and methodology rely on the conditional probability given user u , which is unknown in practice. A direct way would be to estimate the conditional probability using the preference model \mathcal{M} . However, since \mathcal{M} is a complicated neural network, estimating the conditional probabilities through \mathcal{M} is computationally expensive. Additionally, because the preference model is randomly initialized, its estimations can be highly inaccurate, leading to difficulties in convergence or the risk of falling into local optima. Considering the above shortcomings, we employ a trained small model to estimate the conditional probability in our experiments; the specific details will be introduced in the experimental section.

In practice, we optimize the loss using stochastic gradient descent. Since the gradient of term $w \log w + w - 1$ w.r.t. preference score is zero for a given w , it can be disregarded in the practical optimization process. Therefore, the loss function (i.e., Eq. (18)) simplifies to the original multi-class cross-entropy loss multiplied by w . While w should be set as the normalized rectified label \tilde{z} based on our above analysis, we find that optimizing the loss with normalization is difficult and use the unnormalized rectified label \bar{z} in practice. In fact, the unnormalized rectified label can already mitigate the suboptimality, as demonstrated by Eq. (16). The role of normalization is to make the sum of expectations of random variables \tilde{z}_i^j of the j -th layer equal 1, to satisfy the constraints in the theoretical analysis. Normalization actually only influences the learning rate in the stochastic gradient descent compared to the unnormalized label \bar{z} . Note that the normalization coefficients across different layers vary dramatically for a given training instance, but we aggregate the loss of all layers together for optimization, so the normalization will make the optimization difficult in practice due to the difficulty of setting a suitable learning rate. Therefore, we optimize the modified loss with the original rectified label \tilde{z}_i^j without normalization, which can be interpreted as an adaptive adjustment of the learning rate in each layer, and the loss for j -th layer is

$$\tilde{\mathcal{L}}_j(u, y) = -\tilde{z}_{\delta^j(y)}^j \log \left(\frac{\exp o_{\delta^j(y)}^j}{\sum_{k=1}^{N_j} \exp(o_k^j)} \right), \quad (19)$$

and the loss of the whole tree is

$$\tilde{\mathcal{L}}(u, y) = \sum_{j=1}^H \tilde{\mathcal{L}}_j(u, y). \quad (20)$$

4.3 Negative Sampling to Speed Up Training

For the training instance (u, y) , calculating its training loss (i.e., Eq. (20)) requires computing the softmax probability of the positive node at each layer. In practical applications, where the corpus size ranges from millions to billions or even tens of billions, computing softmax probabilities at such scales is extremely inefficient. To promote training efficiency, we employ the sampled softmax technique to estimate the gradient of softmax loss and propose a tree-based sampling method for more accurate gradient estimation.

4.3.1 Unbiased Estimation of Softmax Loss Gradient

Sampled softmax is proposed to approximate full softmax during training [60, 61]. Instead of calculating the training loss of layer j (i.e., Eq. (9)) over all classes, sampled softmax only considers the positive class and M negative classes. These M negative classes are sampled from all the negative classes according to certain sampling distribution Q with replacement. In the following, we use \mathcal{I}_M^j to denote the set of indices of M negative nodes at layer j . Then, the indices of training nodes in layer j is $\mathcal{I}_M^j \cup \{\delta^j(y)\}$ for a given instance (u, y) . For example, if $\delta^j(y) = 2$, $M = 5$ and the negative indices set is $\mathcal{I}_M^j = \{3, 4, 8, 7, 4\}$, this indicates that the 2nd node of layer j is the positive node, the 4th node of layer j is sampled twice, and the other nodes (indexed at 3, 8, 7) are each sampled once.

To reduce the approximation bias, we do not directly use the outputs w.r.t. sampled nodes to approximate the original loss [61]. For $i \in \mathcal{I}_M^j \cup \{\delta^j(y)\}$, a slight adjustment is conducted for each output by

$$\hat{o}_i^j = \begin{cases} o_i^j - \ln(Mq_i^j) & \text{if } i \neq \delta^j(y), \\ o_i^j - \ln(1) & \text{if } i = \delta^j(y) \end{cases} \quad (21)$$

where q_i^j denotes the probability of sampling node n_i^j from the negative nodes of layer j . This adjustment can guarantee that the sampled softmax is unbiased when M is infinite (i.e., $M \rightarrow \infty$) [61]. Then, the loss is calculated over the adjusted outputs, and the training loss Eq. (19) at layer j can be adjusted to

$$\hat{\mathcal{L}}_j(u, y) = -\bar{z}_{\delta^j(y)}^j \log \hat{p}_{\delta^j(y)}^j = -\bar{z}_{\delta^j(y)}^j \log \frac{\exp \hat{o}_{\delta^j(y)}^j}{\sum_{k \in \mathcal{I}_M^j \cup \{\delta^j(y)\}} \exp \hat{o}_k^j}. \quad (22)$$

Previous literature [47, 61] has proved that proper specified sampling distribution Q used in sampled softmax can lead to the unbiased estimation of the gradient for the original loss, i.e., $\mathbb{E}_{\mathcal{I}_M^j \sim Q} \left[\frac{\partial \hat{\mathcal{L}}_j(u, y)}{\partial o_i^j} \right] = \frac{\partial \tilde{\mathcal{L}}_j(u, y)}{\partial o_i^j}$. We state their theorem in a different way so that it can be compatible with our method:

Theorem 2 (Theorem 2.1 of [47]). *The gradient of loss Eq. (22) w.r.t. sampled softmax is an unbiased estimator of the gradient of the loss Eq. (19) w.r.t. full softmax if and only if $q_i^j \propto \exp o_i^j$ holds where $1 \leq i \leq N_j$ and the i -th node isn't a positive node at layer j .*

This theorem indicates that if the sampling probability is proportional to the exponential of the preference w.r.t. the negative node, we can get an unbiased estimation of the training loss gradient. However, it still results in linear time complexity w.r.t. the corpus size, similar to calculating the full softmax, because it requires computing the preference score for every node. To address this problem, previous literature [47, 62] develops kernel-based methods to approximate the full softmax for inner product models. Nonetheless, their kernel-based methods aren't suitable for our approach, as our preference model is a complicated neural network. To reduce the computational complexity while maintaining compatibility with our approach, we propose a tree-based sampling method.

4.3.2 Tree-based Sampling

In many studies, uniform sampling is employed due to its simplicity and efficiency, which also applies to our method, where the negative nodes at each layer can be obtained through a uniform distribution. While uniform sampling possesses many advantageous properties, the uniform distribution often diverges significantly from the exact softmax distribution. To better estimate the gradient of the loss function, it is desirable to use a sampling distribution that closely approximates the exact softmax distribution. In response to this need, we propose a tree-based sampling method, which leverages both the tree index and the preference model to make the sampling distribution closer to the softmax distribution than the uniform distribution.

We elaborate on the proposed tree-based sampling method, which is implemented by modifying the beam search retrieval process (see Algorithm 1). Firstly, during sampling along the tree, only one node is retained at each layer (i.e., we set $k = 1$ in Algorithm 1). Secondly, instead of directly choosing the child node with the highest preference score, we sample one child node for expansion. This sampling-based expansion is performed by local softmax probabilities, calculated based on the preference scores of all child nodes under the current node. Concretely, after expanding node n_i^j , the expanding probability for node $n_c^{j+1} \in \mathcal{C}(n_i^j)$ is:

$$\hat{q}_c^{j+1} = \frac{\exp o_c^{j+1}}{\sum_{k \in \{\delta(n) | n \in \mathcal{C}(n_i^j)\}} \exp o_k^{j+1}}. \quad (23)$$

Then, by expanding one node at each layer, we obtain a sample path through the tree from the root to a leaf. These sampled nodes along this path serve as the negative nodes for their respective layers. Finally, we repeat this sampling process until M negative nodes are obtained for each layer. During the sampling, the sampling probability for node n_i^j is the product of expanding probabilities along the sample path from the root to itself:

$$q_i^j = \prod_{m=0}^j \hat{q}_{\delta(\rho^m(n_i^j))}^m \quad (24)$$

The correctness of the above sampling process can be affirmed by the fact that the sum of sampling probabilities of nodes within the same layer equals 1.

Proposition 4. For any layer j ($0 \leq j \leq H$), the sum of sampling probabilities via tree-based sampling for j -th layer's nodes is exactly 1, i.e.,

$$\sum_{i=1}^{N_j} q_i^j = \sum_{i=1}^{N_j} \prod_{m=0}^j \tilde{q}_{\delta(\rho^m(n_i^j))}^m = 1.$$

The proof of the above proposition is provided in Appendix B.4. Moreover, our proposed sampling method has a lower time complexity, as the number of sampling operations is proportional to the tree height and the sampling probability (i.e., the local softmax probability) can be computed efficiently because it only relies on scores of a limited number of child nodes.

We illustrate the process in Figure 1 to elucidate the tree-based sampling method. The sampling process starts from the root, i.e., node 0. The node 0's child nodes are node 1 and node 2, with expanding probabilities of 0.3 and 0.7, respectively, in this case. Node 1 is sampled for expansion, and the process continues from node 1, repeating until the leaf node 8 is sampled. Finally, the path $0 \rightarrow 1 \rightarrow 3 \rightarrow 8$ is sampled from the tree, and the corresponding sampled negative nodes are $\{1, 3, 8\}$. For any node in the tree, its sampling probability is the product of the expanding probabilities along the path from the root to itself. For example, in Figure 1, the sampling probability for the node 4 is $0.18 = 0.3 \times 0.6$, and for the node 9 is $0.144 = 0.3 \times 0.6 \times 0.8$. Through simple calculation, we can verify that the sum of the probabilities of each node being sampled is exactly 1 for any layer.

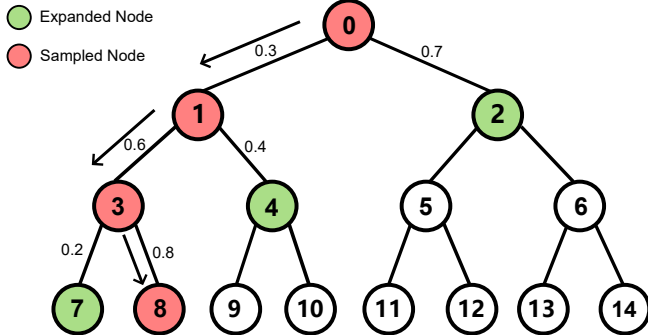


Fig. 1. Illustration of tree-based sampling along the tree. The number beside the edge is the child's expanding probability given the parent.

4.3.3 Theoretical Support

To obtain an unbiased estimation of the gradient for the original training loss, Theorem 2 dictates that the sampling probability for each node should be proportional to the exponential of its preference score. Our proposed tree-based sampling method is grounded in this principle. By leveraging the tree index and the preference model during the sampling process, it directly utilizes the node's local softmax probability for negative sampling, which promotes the sampling distribution closer to the softmax distribution. Furthermore, when the preference scores satisfy certain

conditions, the sampling probability of any node in the tree-based sampling will align precisely with that node's softmax probability, as formalized in the following theorem:

Theorem 3. For any node n_i^j of the tree, if the preference score o_i^j satisfies the following condition:

$$\exp o_i^j \propto \sum_{k \in \{\delta(n) | n \in \mathcal{C}(n_i^j)\}} \exp o_k^{j+1}, \quad (25)$$

and the proportionality coefficients within the same layer are equal, then the sampling probability of node n_i^j in the tree-based sampling equals its softmax probability in layer j , expressed as:

$$q_i^j = \frac{\exp o_i^j}{\sum_{k=1}^{N_j} \exp o_k^j}. \quad (26)$$

Although Theorem 3 imposes a relatively stringent condition that may not be fully satisfied in practical applications, it is noteworthy that optimizing the original multi-class cross-entropy loss can effectively align the score preferences with this condition. Particularly, according to Eq. (12), for the original label z_i^j , we have

$$\mathbb{E}[z_i^j | u] = \sum_{k \in \{\delta(n) | n \in \mathcal{C}(n_i^j)\}} \mathbb{E}[z_k^{j+1} | u].$$

Then, by Lemma 7, as we are optimizing a loss function that can be expressed as Bregman divergence, the optimization leads to the preference score satisfying $g(o^j) = \mathbb{E}[z^j | u]$, where g is the softmax function. Consequently, we obtain:

$$\frac{\exp o_i^j}{\sum_{m=1}^{N_j} \exp o_m^j} = \sum_{k \in \{\delta(n) | n \in \mathcal{C}(n_i^j)\}} \frac{\exp o_k^{j+1}}{\sum_{m=1}^{N_{j+1}} \exp o_m^{j+1}}.$$

Furthermore, we can get:

$$\exp o_i^j \propto \sum_{k \in \{\delta(n) | n \in \mathcal{C}(n_i^j)\}} \exp o_k^{j+1},$$

where $\sum_{m=1}^{N_j} \exp o_m^j / \sum_{m=1}^{N_{j+1}} \exp o_m^{j+1}$ is the proportionality coefficient shared across layer j , satisfying the condition in Theorem 3.

Within the rectification method under beam search, the tree aligns the max-heap in expectation; then, the optimization will lead to the following results:

$$\frac{\exp o_i^j}{\sum_{m=1}^{N_j} \exp o_m^j} = \max_{k \in \{\delta(n) | n \in \mathcal{C}(n_i^j)\}} \frac{\exp o_k^{j+1}}{\sum_{m=1}^{N_{j+1}} \exp o_m^{j+1}},$$

that is,

$$\exp o_i^j \propto \max_{k \in \{\delta(n) | n \in \mathcal{C}(n_i^j)\}} \exp o_k^{j+1},$$

where the proportionality coefficient is still $\sum_{m=1}^{N_j} \exp o_m^j / \sum_{m=1}^{N_{j+1}} \exp o_m^{j+1}$. Since

$$\lambda_i^j \triangleq \frac{\max_{k \in \{\delta(n) | n \in \mathcal{C}(n_i^j)\}} \exp o_k^{j+1}}{\sum_{k \in \{\delta(n) | n \in \mathcal{C}(n_i^j)\}} \exp o_k^{j+1}} \quad (27)$$

is approximately 1 when $\max_{k \in \{\delta(n) | n \in \mathcal{C}(n_i^j)\}} o_k^{j+1}$ is much higher than the preference scores of other child nodes, the

sampling probability remains close to the softmax probability. Specifically, we have the following proposition:

Proposition 5. *For any node n_i^j of the tree, we define its probability bias between its sampling probability q_i^j and softmax probability as follows:*

$$\text{bias}_i^j = q_i^j - \frac{\exp o_i^j}{\sum_{k=1}^{N_j} \exp o_k^j}.$$

Suppose the preference score o_i^j satisfies the following condition:

$$\exp o_i^j \propto \max_{k \in \{\delta(n) | n \in \mathcal{C}(n_i^j)\}} \exp o_k^{j+1}, \quad (28)$$

the proportionality coefficients within the same layer are equal, and $\lambda_i^j \in (1 - \varepsilon, 1)$, where ε is a positive real number that is close to 0. The probability bias of node n_i^j can be controlled as follows:

$$|\text{bias}_i^j| \leq \frac{(j-1)\varepsilon}{1-\varepsilon}. \quad (29)$$

Based on the above proposition, we can further derive the following corollary:

Corollary 1. *For the j -th layer, suppose the preference scores o_i^j ($i \in [N_j]$) are bounded by a constant B_o . The KL divergence between sampling distribution Q^j w.r.t. softmax distribution P^j can be bounded as follows:*

$$D_{KL}(Q^j || P^j) \leq \log \left(1 + B_o^j N_j e^{2B_o} \right), \quad (30)$$

where $B_o^j \triangleq \frac{(j-1)\varepsilon}{1-\varepsilon}$ is the upper bound of the probability bias of nodes in layer j .

The proofs of Theorem 3, Proposition 5 and Corollary 1 are presented in Appendix B.5, Appendix B.6 and Appendix B.7, respectively. Theorem 3 provides valuable insights for designing sampling schemes and justifies the rationality of our proposed tree-based sampling method. Furthermore, Proposition 5 and Corollary 1 demonstrate that this sampling method also applies to the rectification method under beam search. It can be observed that when ε is small, the difference between the sampling distribution and softmax distribution is also small, leading to a more accurate estimation of the softmax loss gradient.

4.4 Tree Index Updating

Without sufficient domain knowledge, initializing a well-structured tree is challenging. Even if the preference model converges during training, it can only adapt to the current, potentially suboptimal tree. Consequently, it is necessary to update the tree index alongside the optimization of the preference model. In this section, we introduce how to update the tree index (i.e., updating the mapping π) when keeping the preference model fixed.

At first, we employ a method similar to TDM and JTM to construct the initial tree. The tree is used to represent the user interests' hierarchical information so that similar items should be organized in close positions on the last layer of the tree. It's natural to rely on the category information of items to build the initial tree. Firstly, we shuffle all the categories and put the items together if they share the same category

ID. If an item belongs to more than one category, a random one is assigned to the item for uniqueness. Secondly, the items within each category are recursively divided into two equal parts until each partition contains only one item. In this way, we can construct a near-complete binary tree from the root node to the leaf node. A simple balancing strategy can be used to adjust the tree. Specifically, for leaf nodes not at the deepest level, an internal node is repeatedly inserted between the leaf and its parent until all leaf nodes are positioned at the same depth. We use a binary tree in our experiments. In fact, any n-ary tree can be constructed in such a way by partitioning each cluster into more nearly equal parts at each iteration.

Tree index updating is still based on the training set $S = \{(u_i, y_i)\}_{i=1}^m$. We partition S into different user-item pair sets, denoted by $\mathcal{A}_y = \{(u_i, y_i) | y_i = y\}$, where \mathcal{A}_y consists of all user-item pairs for which the item is exactly y . Given the old mapping π and each user-item pair set \mathcal{A}_y , we fix the preference model and assign each item to the tree nodes step by step, from the root node to the leaf nodes, to obtain the new mapping π' .

All items are initially assigned to the root node, i.e., current level $j = 0$. Then, we try to assign them to the nodes at level $j' \triangleq \min(H, j+d)$. Here, the hyperparameter d determines the number of layers to skip during the allocation process along the tree, where the purpose of skipping layers is to accelerate the allocation and, to some extent, prevent items from being assigned to the inappropriate leaf node due to early incorrect allocation. For an item y initially assigned to the root node, it must be reassigned to one of the nodes at level j' . Since we are using a binary tree, there will be $c \leq 2^d$ candidate nodes. Without loss of generality, we denote these candidate nodes as $n_1^{j'}, n_2^{j'}, \dots, n_c^{j'}$. The preference of user u for node $n_i^{j'}$ ($1 \leq i \leq c$) is denoted as $o_i^{j'}$ and is calculated by the fixed preference model. We define the matching score between item y and node $n_i^{j'}$ ($1 \leq i \leq c$) as follows:

$$\text{Score}(y, n_i^{j'}) = \sum_{(u, y) \in \mathcal{A}_y} \log \frac{\exp o_i^{j'}}{\sum_{k=1}^c \exp o_k^{j'}}. \quad (31)$$

The above matching score represents the log-likelihood of assigning item y to node $n_i^{j'}$, calculated based on \mathcal{A}_y and the fixed preference model. A higher score indicates a greater suitability for allocating the item to the corresponding node. Then, we rank the c scores and assign y to the node with the highest matching score. All items are disjointly assigned to the nodes at level j' , where the number of items assigned to the node $n_i^{j'}$ equals the number of leaf nodes within the subtree rooted at $n_i^{j'}$. If the number of assigned items exceeds the limitation, y is reassigned to the node with the second-highest matching score, or to subsequent nodes in descending order of matching scores, until the assignment satisfies the limit. In this way, we can assign each item belonging to the root initially to a node at level j' . Now, we regard $n_1^{j'}, \dots, n_c^{j'}$ as root nodes of c subtrees and repeat the process recursively to assign the items to deeper layers until each leaf node is assigned an item. Finally, we can get the new mapping π' . To compute the matching score (i.e., Eq. (31)), we need to compute the denominator $\sum_{k=1}^c \exp o_k^{j'}$, so

the number d need to be small to fit the time complexity and computational resource; in our experiments, we set $d = 7$.

To illustrate the tree update process, Figure 2 presents an example with eight items labeled a to h and a step $d = 2$. Initially, all items are at the root node. We need to allocate items to the layer at a distance of 2 from the root. This layer consists of four nodes, with each node receiving two items. According to the matching scores, item f should ideally be assigned to node 4, which has the highest matching score. However, since node 4 already contains two items (b and c), item f is reallocated to node 5, which has the next highest score. Once allocation in the second layer is complete, the process continues to deeper layers. As the leaf nodes are located in the third layer, just one step from the second layer (less than d), items are directly assigned to the third layer. Ultimately, each leaf node is allocated one item, completing the tree update.

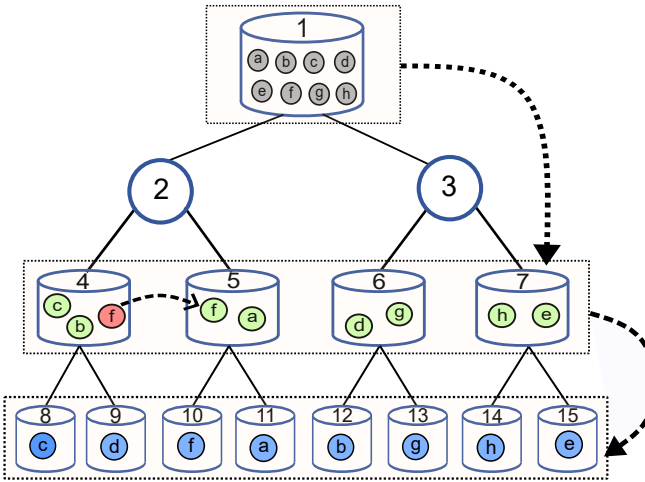


Fig. 2. The process of updating the mapping between items and leaf nodes, where $d = 2$ in this case.

In fact, our tree learning strategy assigns items to tree nodes in a top-down manner, which can also be viewed as a hierarchical clustering from coarse grain to fine grain, and d controls the grain size. The main difference between ours and the one in JTM is the calculation of matching scores. Both JTM and our method compute the log-likelihood as the matching score, but while JTM directly sums up the binary classification probabilities for this calculation, our strategy relies on the softmax-based multi-class probabilities, which is compatible with our training mode.

5 GENERALIZATION ANALYSIS

In this section, we provide a generalization analysis of the deep tree-based retriever, to offer a comprehensive theoretical understanding of our proposed method. Our analysis employs Rademacher complexity to derive a data-dependent generalization error bound of the tree model, which is optimized using the modified loss with rectified labels alongside the sampled softmax technique, demonstrating its great generalization capability.

The variation of DIN is used as the preference model, which is formalized in Section 3.2.2. Suppose the norm of

the weight matrix is bounded, we can get such function space for the model:

$$\begin{aligned} \mathcal{M} = \{f : (u, n) \mapsto f_{\text{DIN}}(u, n) \mid \|\mathbf{w}_n\|_2 \leq B_0, \forall n \in \mathcal{N}; \\ \|\mathbf{W}_k\|_1 \leq B_1, \forall k \in [L]; \|\mathbf{W}_w^{(j)}\| \leq B_2, \forall j \in 1, 2\}. \end{aligned} \quad (32)$$

Lemma 2 (Rademacher Complexity of DIN). *Suppose $\forall u \in \mathcal{U}$, $\forall k \in [K]$, $\|\mathbf{a}_k^{(u)}\|_2 \leq B_a$, then the Rademacher complexity of \mathcal{M} can be bounded as follows:*

$$\widehat{\mathcal{R}}_m(\mathcal{M}) \leq \frac{2c_\phi^{L-1}B_1^L(B_0 + KB_{w_1} + KB_{w_2}\tau)}{\sqrt{m}}, \quad (33)$$

where $B_{w_1} = c_\phi^2 B_2^2 B_a^2$, $B_{w_2} = c_\phi^2 B_0 B_2^2 (B_a^2 + B_a)$, and $\tau = \sqrt{(2B-1)|\mathcal{Y}|}/\sqrt{B-1}$.

The proof of Lemma 2 is provided in Appendix B.8. With the Rademacher complexity of the DIN model, we now derive the generalization bound for the modified loss with rectified labels (i.e., Eq. (20)) in Section 4.2. Since the overall loss for the tree is the sum of the losses at each layer, we begin by examining the generalization bound for the loss at the j -th layer. The result is presented as follows:

Lemma 3. *Suppose the function in \mathcal{M} is bounded by a constant $B_{\mathcal{M}}$, the following inequality holds with a probability of at least $1 - \delta$:*

$$\begin{aligned} \mathbb{E}_{(u, y) \sim \mathbb{P}} [\widetilde{\mathcal{L}}_j(u, y)] &\leq \frac{1}{m} \sum_{i=1}^m \widetilde{\mathcal{L}}_j(u_i, y_i) \\ &+ 8N_j \frac{c_\phi^{L-1}B_1^L(B_0 + KB_{w_1} + KB_{w_2}\tau)}{\sqrt{m}} \\ &+ (4 \log N_j + 8B_{\mathcal{M}}) \sqrt{\frac{2 \log (4/\delta)}{m}}. \end{aligned} \quad (34)$$

The theoretical analysis presented above demonstrates the generalization capacity of the proposed method of optimizing the preference model, where the objective is to minimize a modified softmax loss with rectified labels. In practice, however, the sampled softmax is employed to speed up optimization as detailed in Section 4.3. To ensure theoretical analysis is consistent with our proposed method, we incorporate the bias introduced by the sampled softmax loss w.r.t. the softmax loss into the theoretical result. For a given instance (u, y) , the model \mathcal{M} outputs N_j preference scores for nodes at j -th layer, forming a logit vector $\mathbf{o}^j \in \mathbb{R}^{N_j}$. Suppose the i -th node is positive (i.e., $i = \delta^j(y)$) while the others are negative, the softmax loss for layer j is given by:

$$\ell_{\text{softmax}}^j(u, y) = -\log \frac{\exp o_i^j}{\sum_{k=1}^{N_j} \exp o_k^j}.$$

A set of indices of M negative nodes, denoted by \mathcal{I}_M^j , is sampled according to a sampling distribution $Q^j(u, y)$, where u and y specify that the distribution depends on the instance (u, y) . For simplicity, we omit u and y , and use the notation Q^j . The adjusted logit vector $\hat{\mathbf{o}}^j$ is computed according to \mathbf{o}^j and Q^j as specified in Eq. (21). Then, the sampled softmax loss for layer j is calculated as follows:

$$\ell_{\text{sampled-softmax}}^j(u, y, \mathcal{I}_M^j) = -\log \frac{\exp \hat{o}_i^j}{\sum_{i' \in \mathcal{I}_M^j \cup \{i\}} \exp \hat{o}_{i'}^j}.$$

The bias of the sampled softmax loss w.r.t. the softmax loss is presented as follows:

Lemma 4. For any given instance (u, y) and the j -th layer, the softmax loss can be bounded by the sum of two terms: the expectation of the sampled softmax loss over \mathcal{I}_M^j and the KL divergence between Q^j w.r.t. P^j . It is expressed as follows:

$$\ell_{\text{softmax}}^j(u, y) \leq \mathbb{E}_{\mathcal{I}_M^j} \left[\ell_{\text{sampled-softmax}}^j(u, y, \mathcal{I}_M^j) \right] + D_{\text{KL}}(Q^j \| P^j),$$

where $P^j(u, y)$ is the softmax distribution in the layer j for the instance (u, y) , with i -th node's softmax probability defined as $p_i^j \triangleq \exp o_i^j / \sum_{k=1}^{N_j} \exp o_k^j$.

Then, combine Lemma 2, Lemma 3 and Lemma 4, and aggregate from the 1st layer to the H -th layer, we can get following result:

Theorem 4. The following inequality holds with a probability of at least $1 - \delta$:

$$\begin{aligned} \mathbb{E}_{(u,y) \sim \mathbb{P}} \left[\tilde{\mathcal{L}}(u, y) \right] &\leq \frac{1}{m} \sum_{i=1}^m \sum_{j=1}^H \hat{\mathcal{L}}_j(u_i, y_i) \\ &+ \sum_{j=1}^H \mathbb{E}_{(u,y) \sim \mathbb{P}} \left[D_{\text{KL}}(Q^j \| P^j) \right] \\ &+ 8\tau^2 \frac{c_{\phi}^{L-1} B_1^L (B_0 + K B_{w_1} + K B_{w_2} \tau)}{\sqrt{m}} \\ &+ \left(8 \log(\tau) + 8HB_M \right) \sqrt{\frac{2 \log(4/\delta)}{m}}. \end{aligned} \quad (35)$$

Theorem 4 provides a comprehensive theoretical analysis of our proposed method. As shown in Eq. (35), the left side of the inequality is the expected risk of the modified loss with rectified labels. Minimizing this risk results in optimal outcomes under beam search, as detailed in Section 4.2. On the inequality's right side, the first term corresponds to the empirical loss optimized in practice. The second term is the expected KL divergence of the negative sampling distribution w.r.t. the softmax distribution at each layer. It can be observed that the closer the negative sampling distribution is to the softmax distribution, the lower the generalization risk. As shown in Corollary 1, the KL divergence can be effectively controlled in our proposed tree-based sampling, providing insight into why it performs well from a generalization perspective. The third term captures the influence of model parameters and tree structure on generalization risk. Notably, when the number of items (i.e., $|\mathcal{Y}|$) is fixed, increasing the number of branches B results in a smaller τ , leading to a tighter generalization bound. Moreover, when the sample size m is sufficiently large, the last two terms tend to vanish, meaning that with enough data, the generalization risk can be effectively controlled by the empirical loss and the KL divergence.

6 EXPERIMENTS

We conduct a series of experiments designed to answer the following research questions related to the joint optimization framework of preference models and tree indexes: **RQ-1:** Is the softmax-based multi-class classification training mode more suitable than the binary classification training mode for the tree model? **RQ-2:** Is the modified loss with rectified labels

effective in mitigating the suboptimality of the multi-class cross-entropy loss under beam search in practice? **RQ-3:** Does the proposed sampling method, guided by the sampled softmax theory to mitigate the approximation bias, prove to be effective? **RQ-4:** Can the DTR learn a reasonable mapping relationship between items and leaf nodes? **RQ-5:** Does the performance of the proposed sampling method fluctuate with the number of negative samples?

6.1 Datasets

The experiments are conducted on the four real-world datasets¹: Movie Lens 10M (abbreviated as Movie), MIND Small Dev (abbreviated as MIND), Amazon Books (abbreviated as Amazon), Tmall Click (abbreviated as Tmall). Movie is a public film rating dataset, MIND is a news recommendation dataset collected by Microsoft, Amazon is a dataset documenting book purchases and ratings on the Amazon e-commerce site, Tmall records the shopping behaviors of users on Alibaba's Tmall marketplace. We process all datasets into a form of implicit feedback, where interactions between users and items are marked as 1, and non-interactions as 0. Additionally, users with fewer than 15 interactions were filtered out, with the post-filtering data statistics presented in Table 1. For each dataset, 10% of users are randomly selected as validation users, 10% as test users, and all remaining users as training users. For training users, each interaction sequence is constrained to the most recent 70 interactions, with shorter sequences padded with zeros. The first 69 interactions serve as input, while the 70th is used as the label. For validation and test users, the first half of their interaction history is used as input, with the second half serving as labels for prediction.

TABLE 1
Statistics of datasets

Dataset	#User	#Item	#Interaction	Density
Movie	69,878	10,677	10,000,054	1.34%
MIND	36,281	7,129	5,610,960	2.16%
Amazon	29,980	67,402	2,218,926	0.11%
Tmall	139,234	135,293	10,487,585	0.05%

6.2 Baselines

We compared the proposed DTR with other related algorithms, which fall into two broad categories: 1) models that employ brute-force search without indexing and 2) tree-based models similar to DTR. It should be noted that the former requires a significant amount of time to perform retrieval; comparing them with index-based retrieval models is not fair, and their results are only used as a reference. The introductions of these algorithms are as follows:

- Item-CF [63] is a basic collaborative filtering algorithm and is widely used in recommendation tasks.
- DIN [1] employs an attention mechanism to capture the user preference for items from the user's interaction history. Since it cannot be used for efficient recommendation directly, the performance based on brute-force search is reported as a reference metric.

1. <https://drive.google.com/drive/folders/1ahiLmzU7cGRPx5qGMqtAChte2eYp9gI>

- YouTubeDNN [64] utilizes inner products to compute user preference scores. Once the user and item embeddings are learned, the recommendation task is transformed into a Maximum Inner Product Search (MIPS). We use the implementation provided by DeepMatch² and report the results obtained through brute-force search.
- PLT [65] organizes items into a label tree, where each node represents a conditional probability estimator. The probability of an item is determined by multiplying the probabilities estimated along the path from the root to the corresponding leaf. Recommendations are then made based on the calculated probability.
- TDM [11] is a tree-based recommendation model proposed by Alibaba Group. It simultaneously learns the preference model and the tree-index structure, using beam search during inference to perform efficient recommendation.
- JTM [12] is an enhanced version of TDM. It introduces a method for jointly learning the index structure and the user preference prediction model.
- OTM [54] mitigates the training-testing discrepancies of tree models under beam search by sampling negative nodes through beam search and correcting the pseudo-labels of nodes during training. It is a state-of-the-art tree model.

6.3 Metric

To evaluate the performance of the retrieval model, we use *Precision@K*, *Recall@K*, and *F-measure@K* as the evaluation criteria. Suppose $\mathcal{P}(u)$ ($|\mathcal{P}(u)| = K$) denotes the set of items retrieved by the model for user u , and $\mathcal{G}(u)$ represents the set of items that the user has interacted with, i.e., the ground truth associated with user u . For user u , the evaluation metrics *Precision@K* and *Recall@K* are calculated as follows:

$$\text{Precision}@K(u) = \frac{|\mathcal{P}(u) \cap \mathcal{G}(u)|}{K},$$

$$\text{Recall}@K(u) = \frac{|\mathcal{P}(u) \cap \mathcal{G}(u)|}{|\mathcal{G}(u)|},$$

and *F-measure@K* is calculated as follows:

$$\text{F-measure}@K(u) = \frac{2 \cdot \text{Precision}@K(u) \cdot \text{Recall}@K(u)}{\text{Precision}@K(u) + \text{Recall}@K(u)}.$$

6.4 Settings

We provide detailed settings of the baseline algorithm and our algorithm.

For Item-CF, the number of neighbors is set to 500 for the Movie, MIND and 1000 for Amazon, Tmall, respectively. The cosine similarity coefficient is employed to measure the similarity between items. DIN comprises an embedding layer followed by an MLP with layer sizes [128,64,2], which outputs the probability of a user liking a given item. YouTubeDNN also includes an embedding layer and an MLP with layer sizes [128,64,24], and the number of negative samples is set to 1,000.

2. <https://github.com/shenweichen/DeepMatch>

For all tree-based algorithms, a binary tree is selected as the tree index (i.e., B is set to 2), and the DIN model or its variance is used as the preference score model. The first 69 interactions in the sequence are segmented using 10 sliding windows, with the number of interactions in each window being [20, 20, 10, 10, 2, 2, 2, 1, 1, 1] respectively. For all tree-based algorithms, except for OTM, the same tree structure initialized based on item categories is used, whereas OTM employs a tree structure learned from JTM as described in [54]. TDM, JTM, and DTR include a process for updating the tree index. Due to the instability associated with tree updating in TDM, it is configured to include only 4 iterations of tree updating, while JTM and DTR are set to include 12 iterations each. Negative nodes are the sibling nodes of the positive node in PLT, while for other tree-based algorithms, the negative nodes are sampled from the same layer as the positive node in each layer. For TDM and JTM, the number of negative samples per layer is set to 6, 3, 5, and 6 for the Movie, MIND, Amazon, and Tmall datasets, respectively. In OTM, since sampled nodes are the candidates generated from the beam search process, the number of samples is set to $2k$, where k is the beam size. For DTR, the number of negative samples is set to 70.

DTR employs two sampling methods: uniform sampling and tree-based sampling, denoted as DTR(U) and DTR(T), respectively. DTR(T) further incorporates the modified loss with rectified labels, referred to as DTR(T-RL). For DTR(T-RL), we need to use a trained small model to estimate the conditional probability. SASRec is selected as the estimator. For a given user u , the historical sequence is input into SASRec to generate a semantic vector, which is then used to compute the inner product with each item embedding. Subsequently, the inner products across the entire item set are processed through a softmax function to obtain the conditional probabilities. We train SASRec with the same trainset as other algorithms. When evaluated on the test-set, the trained SASRec performs at most 0.8% lower than DTR(T) in terms of *F-measure@20* across four datasets, indicating that it is a well-behaved estimator. Notice that SASRec is a two-tower model, so the additional computation required for probability estimation is relatively minimal. In our experiments, the time spent on estimating probabilities accounts for approximately 17.5% to 22.6% of the total time across four datasets, which is considered acceptable.

In all algorithms, the dimension of the item embedding is set to 24, and the batch size is set to 100. We employ Adam as the optimizer [66], with a learning rate initialized at 1.0e-3 and subjected to exponential decay. For the tree-based algorithms, the beam size k is set to 150, i.e., we select at most 150 items to expand when we conduct a beam search along the tree. All experiments are conducted on a Linux server equipped with a 3.00 GHz Intel CPU, 300 GB of main memory, and NVIDIA 20/30 series GPUs.

6.5 Comparison with baselines

The experiment results are shown in Table 2. In the table, the best performance of tree-based algorithms is highlighted in bold. Additionally, any results from brute-force search algorithms that exceed the best performance of tree-based algorithms are also emphasized in bold for reference. Based on the results, we can make the following findings:

TABLE 2
Experimental results for different algorithms across four datasets.

Dataset	Algorithm	top-K=20			top-K=40			top-K=60		
		Precision	Recall	F-measure	Precision	Recall	F-measure	Precision	Recall	F-measure
Movie	Item-CF	0.1058	0.0508	0.0600	0.1211	0.1218	0.1037	0.1266	0.1886	0.1292
	DIN	0.2132	0.1142	0.1309	0.1957	0.2013	0.1706	0.1807	0.2685	0.1848
	YoutubeDNN	0.2043	0.1113	0.1270	0.1874	0.1924	0.1630	0.1746	0.2560	0.1770
	PLT	0.1606	0.0859	0.0981	0.1478	0.1489	0.1264	0.1385	0.2006	0.1389
	TDM	0.1901	0.1012	0.1159	0.1741	0.1770	0.1499	0.1624	0.2383	0.1641
	JTM	0.2141	0.1169	0.1335	0.1922	0.1993	0.1682	0.1770	0.2650	0.1815
	OTM	0.2321	0.1290	0.1470	0.2009	0.2086	0.1767	0.1822	0.2687	0.1862
	DTR(U)	0.2367	0.1231	0.1431	0.2054	0.2032	0.1759	0.1842	0.2616	0.1850
	DTR(T)	0.2511	0.1343	0.1546	0.2135	0.2169	0.1853	0.1893	0.2772	0.1924
	DTR(T-RL)	0.2545	0.1374	0.1580	0.2176	0.2240	0.1905	0.1936	0.2876	0.1985
Mind	Item-CF	0.2243	0.1218	0.1416	0.1962	0.1977	0.1740	0.1769	0.2518	0.1833
	DIN	0.4174	0.1912	0.2320	0.3485	0.2930	0.2756	0.3042	0.3634	0.2861
	YoutubeDNN	0.4025	0.1850	0.2243	0.3357	0.2851	0.2671	0.2936	0.3541	0.2775
	PLT	0.2341	0.0927	0.1168	0.2024	0.1532	0.1494	0.1818	0.2011	0.1626
	TDM	0.3156	0.1365	0.1687	0.2706	0.2236	0.2116	0.2375	0.2832	0.2225
	JTM	0.3457	0.1547	0.1892	0.2806	0.2354	0.2213	0.2432	0.2925	0.2288
	OTM	0.3724	0.1609	0.1978	0.3144	0.2523	0.2404	0.2785	0.3188	0.2544
	DTR(U)	0.3904	0.1804	0.2188	0.3063	0.2621	0.2448	0.2612	0.3191	0.2482
	DTR(T)	0.4044	0.1853	0.2250	0.3318	0.2808	0.2634	0.2889	0.3472	0.2726
	DTR(T-RL)	0.4210	0.1938	0.2350	0.3401	0.2869	0.2695	0.2957	0.3544	0.2787
Amazon	Item-CF	0.0175	0.0178	0.0169	0.0284	0.0554	0.0360	0.0314	0.0860	0.0440
	DIN	0.0706	0.0495	0.0528	0.0605	0.0828	0.0625	0.0536	0.1080	0.0641
	YoutubeDNN	0.0606	0.0399	0.0436	0.0522	0.0682	0.0527	0.0470	0.0910	0.0553
	PLT	0.0238	0.0147	0.0162	0.0201	0.0245	0.0193	0.0181	0.0321	0.0202
	TDM	0.0514	0.0333	0.0365	0.0419	0.0530	0.0416	0.0361	0.0674	0.0418
	JTM	0.0606	0.0411	0.0444	0.0507	0.0674	0.0517	0.0452	0.0892	0.0537
	OTM	0.0704	0.0440	0.0486	0.0584	0.0710	0.0566	0.0514	0.0923	0.0583
	DTR(U)	0.0709	0.0502	0.0535	0.0594	0.0820	0.0619	0.0521	0.1067	0.0630
	DTR(T)	0.0757	0.0517	0.0557	0.0613	0.0829	0.0631	0.0533	0.1073	0.0639
	DTR(T-RL)	0.0777	0.0542	0.0580	0.0626	0.0847	0.0644	0.0544	0.1093	0.0651
Tmall	Item-CF	0.0093	0.0084	0.0083	0.0181	0.0314	0.0216	0.0205	0.0498	0.0273
	DIN	0.0488	0.0350	0.0376	0.0379	0.0531	0.0405	0.0322	0.0665	0.0397
	YoutubeDNN	0.0331	0.0211	0.0236	0.0276	0.0349	0.0278	0.0243	0.0457	0.0287
	PLT	0.0167	0.0111	0.0122	0.0133	0.0176	0.0137	0.0114	0.0224	0.0137
	TDM	0.0310	0.0209	0.0229	0.0253	0.0335	0.0262	0.0220	0.0433	0.0266
	JTM	0.0394	0.0275	0.0298	0.0315	0.0427	0.0331	0.0269	0.0538	0.0327
	OTM	0.0459	0.0283	0.0318	0.0361	0.0433	0.0353	0.0307	0.0546	0.0353
	DTR(U)	0.0442	0.0312	0.0337	0.0356	0.0489	0.0377	0.0308	0.0623	0.0376
	DTR(T)	0.0464	0.0329	0.0355	0.0364	0.0503	0.0385	0.0312	0.0634	0.0382
	DTR(T-RL)	0.0482	0.0342	0.0369	0.0373	0.0514	0.0395	0.0317	0.0644	0.0388

- The proposed DTR algorithm consistently outperforms both TDM and JTM across all four datasets. When compared to their enhanced version, OTM, DTR remains highly effective: DTR(U) outperforms OTM in most cases, while DTR(T) and DTR(T-RL) consistently surpass OTM. For example, considering *F-measure*@20, DTR(T-RL) shows improvements of 7.48%, 18.81%, 19.34%, and 16.03% across the four datasets compared to OTM. This result demonstrates that the softmax-based multi-class classification training mode is better suited for jointly optimizing the preference model and tree structure index than the binary classification training mode of TMD, JTM, and OTM, effectively answering **RQ-1**.
- The superiority of DTR(T-RL) over DTR(U) is consistently observed across all datasets. For example, in terms of *F-measure*@20, DTR(T-RL) achieves improvements of 2.20%, 4.44%, 4.13%, and 3.94%, respectively, across the four datasets. This outcome is in line with the theoretical insights discussed in Sections 4.1.2 and 4.2. It confirms that the modified loss function with rectified labels effectively mitigates the suboptimality of the multi-class cross-entropy loss when applied under beam search conditions, thus providing an effective answer to **RQ-2**.
- The performance of DTR(T) consistently surpasses that of DTR(U). For instance, when the top-K value is set to 20, DTR(T) shows an increase in *F-measure* by 8.04%, 2.83%, 4.11%, and 4.41% across the four datasets, respectively. These improvements suggest that the proposed tree-based sampling method more effectively aligns with the requirements of sampled softmax theory, as its sampling probabilities are more closely aligned with the actual softmax probabilities. This result validates the theoretical analysis presented in Section 4.3.3 (i.e., Theorem 3), and effectively addresses **RQ-3**.
- Compared with brute-force search retrieval algorithms, DTR(T-RL) continues to demonstrate strong performance. It outperforms YouTubeDNN across all four datasets and surpasses DIN on the Movie and Amazon datasets. This observation suggests that joint optimization of the index and preference model can exhibit superior performance compared to optimizing them independently. Moreover, with the help of the tree index structure, the preference model can

exclude some distracting items in certain scenarios, thereby enhancing retrieval performance.

6.6 Effectiveness of Tree Index Updating

We demonstrate the effectiveness of the tree index updating strategy employed in DTR, i.e., the validity of updating the mapping relationships between the tree's leaf nodes and items. We illustrate how $F\text{-measure}@20$ changes with updates to the tree index across four datasets. Since PLT and OTM do not involve tree updating, and JTM is an enhanced version of TDM with a tree updating strategy that better aligns with the preference model, we mainly compare JTM and the three variations of DTR in this subsection.

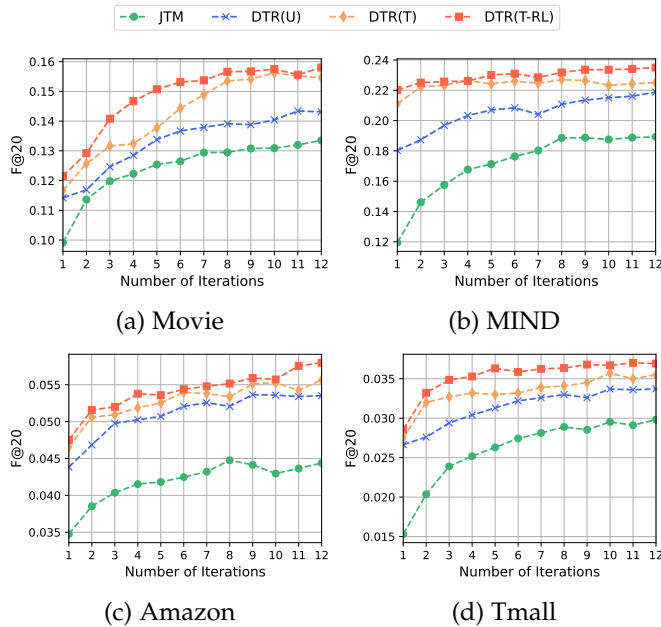


Fig. 3. The variation of $F\text{-measure}@20$ with tree updating across four algorithms.

The experimental results are presented in Figure 3. From these results, the following findings can be made:

- The three variations of DTR consistently show an initial increase followed by a gradual convergence across four different datasets. This phenomenon suggests that the tree update strategy utilized by DTR is effective in establishing a reasonable mapping between items and the tree's leaf nodes. Consequently, the index structure evolves alongside the preference model, leading to improved retrieval performance. This result convincingly addresses **RQ-4**.
- The three variations of DTR consistently exhibit superior performance, significantly outperforming JTM across four datasets. This result further illustrates the superiority of the softmax-based multi-class classification training mode employed by DTR over the binary classification training mode used by JTM, thereby answering **RQ-1** once again.
- Compared to DTR(T), DTR(T-RL) consistently offers advantages during the tree updating process. This phenomenon further demonstrates that the modified loss function, incorporating the rectified label, can

effectively enhance the retrieval performance of the tree-based model, aligning with our theoretical analysis and also answering **RQ-2**.

- The variation of DTR based on tree-based sampling consistently outperforms the one based on uniform sampling. This result indicates that tree-based sampling can estimate the softmax gradient with greater accuracy compared to uniform sampling. It validates the proposed sampling method's rationality and echoes the theoretical conclusions underpinning tree-based sampling, also addressing **RQ-3**.

6.7 Sensitivity w.r.t. Number of Negative Samples

We analyze the impact of the number of negative samples on retrieval performance for our proposed DTR and its variations. We demonstrate how the $F\text{-measure}@20$ varies with the number of negative samples, which ranges from 10 to 90 in increments of 10. All experiments in this subsection are conducted on the initial tree constructed based on the item categories.

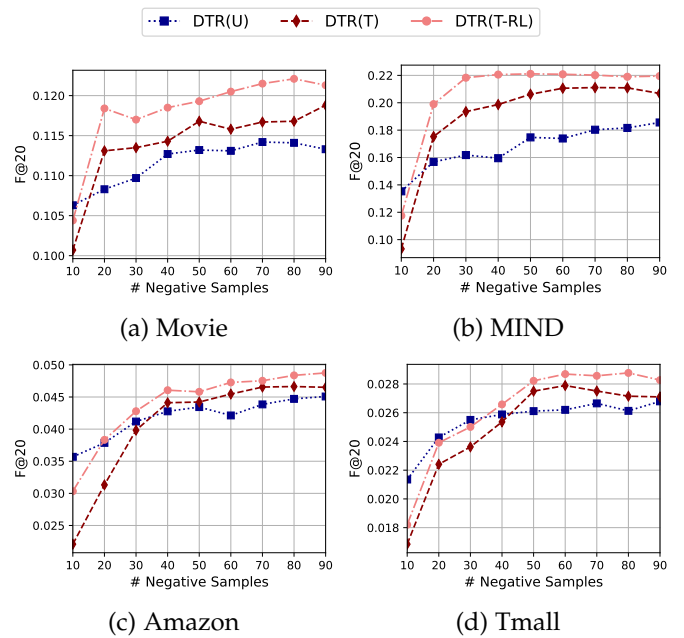


Fig. 4. The $F\text{-measure}@20$ of DTR with varying numbers of negative samples across four datasets.

The experimental results are shown in Figure 4. It can be observed that DTR(U) performs quite well compared to the other two variations based on tree-based sampling when the number of negative samples is relatively small. However, when the negative sample size becomes relatively large, the other two variations consistently outperform DTR(U). It indicates that while uniform sampling is effective due to its good exploration ability, tree-based sampling becomes significantly advantageous with larger sample sizes by leveraging a sampling distribution closer to the softmax distribution, leading to a more accurate estimation of the gradient of the original loss. Moreover, DTR(T-RL) outperforms DTR(T) consistently across four datasets, which validates the effectiveness of the modified loss with rectified labels again. As the number of negative samples increases, the $F\text{-measure}@20$ values of the three variations of DTR

all show a gradual improvement and eventually converge. When the number of negative samples reaches 50 or more, the performance of all three DTR variations stabilizes, indicating that DTR's performance is relatively unaffected by the number of negative samples. This effectively addresses **RQ-5**, confirming that our proposed DTR is insensitive to the number of negative samples once it reaches a suitable threshold.

7 CONCLUSION

The existing tree-based recommendation systems treat the preference model training task as independent binary classification problems for each node. Their training mode suffers from the gap between training and prediction due to the lack of competition among nodes at the same layer. To address this problem, we develop a layer-wise training mode that frames the training task as a softmax-based multi-class classification problem and propose a tree learning method compatible with this training mode. Our theoretical analysis reveals the suboptimality of this training mode under beam search, promoting us to propose a rectification method. Given the significant time cost of calculating softmax probabilities with large-scale datasets, we develop a tree-based sampling method guided by the sampled softmax theory to estimate the loss gradient accurately, thus accelerating the training process. Finally, we provide a generalization analysis of the deep tree-based retriever, demonstrating its great generalization capability. Experimental results validate the effectiveness of our proposed methods.

ACKNOWLEDGMENTS

The work was supported by grants from the National Natural Science Foundation of China (No. 62022077).

REFERENCES

- [1] G. Zhou, X. Zhu, C. Song, Y. Fan, H. Zhu, X. Ma, Y. Yan, J. Jin, H. Li, and K. Gai, "Deep interest network for click-through rate prediction," in *Proceedings of the 24th ACM SIGKDD International Conference on Knowledge Discovery & Data Mining*, 2018, pp. 1059–1068.
- [2] G. Zhou, N. Mou, Y. Fan, Q. Pi, W. Bian, C. Zhou, X. Zhu, and K. Gai, "Deep interest evolution network for click-through rate prediction," in *Proceedings of the AAAI conference on artificial intelligence*, vol. 33, no. 01, 2019, pp. 5941–5948.
- [3] X. He, L. Liao, H. Zhang, L. Nie, X. Hu, and T.-S. Chua, "Neural collaborative filtering," in *Proceedings of the 26th international conference on world wide web*, 2017, pp. 173–182.
- [4] H. Wang, N. Wang, and D.-Y. Yeung, "Collaborative deep learning for recommender systems," in *Proceedings of the 21th ACM SIGKDD international conference on knowledge discovery and data mining*, 2015, pp. 1235–1244.
- [5] F. Zhang, N. J. Yuan, D. Lian, X. Xie, and W.-Y. Ma, "Collaborative knowledge base embedding for recommender systems," in *Proceedings of the 22nd ACM SIGKDD international conference on knowledge discovery and data mining*, 2016, pp. 353–362.
- [6] Y. A. Malkov and D. A. Yashunin, "Efficient and robust approximate nearest neighbor search using hierarchical navigable small world graphs," *IEEE transactions on pattern analysis and machine intelligence*, vol. 42, no. 4, pp. 824–836, 2018.
- [7] H. Jegou, M. Douze, and C. Schmid, "Product quantization for nearest neighbor search," *IEEE Transactions on Pattern Analysis and Machine Intelligence*, vol. 33, no. 1, pp. 117–128, 2011.
- [8] A. Babenko and V. Lempitsky, "Additive quantization for extreme vector compression," in *Proceedings of CVPR'14*, 2014, pp. 931–938.
- [9] R. Guo, P. Sun, E. Lindgren, Q. Geng, D. Simcha, F. Chern, and S. Kumar, "Accelerating large-scale inference with anisotropic vector quantization," in *International Conference on Machine Learning*. PMLR, 2020, pp. 3887–3896.
- [10] Z. Li, J. Tang, L. Zhang, and J. Yang, "Weakly-supervised semantic guided hashing for social image retrieval," *International Journal of Computer Vision*, vol. 128, no. 8, pp. 2265–2278, 2020.
- [11] H. Zhu, X. Li, P. Zhang, G. Li, J. He, H. Li, and K. Gai, "Learning tree-based deep model for recommender systems," in *Proceedings of the 24th ACM SIGKDD International Conference on Knowledge Discovery & Data Mining*, ser. KDD '18. New York, NY, USA: Association for Computing Machinery, 2018, p. 1079–1088.
- [12] H. Zhu, D. Chang, Z. Xu, P. Zhang, X. Li, J. He, H. Li, J. Xu, and K. Gai, "Joint optimization of tree-based index and deep model for recommender systems," in *NeurIPS*, 2019.
- [13] C. Feng, D. Lian, Z. Liu, X. Xie, L. Wu, and E. Chen, "Forest-based deep recommender," in *Proceedings of the 45th International ACM SIGIR Conference on Research and Development in Information Retrieval*, 2022, pp. 523–532.
- [14] M. Datar, N. Immorlica, P. Indyk, and V. S. Mirrokni, "Locality-sensitive hashing scheme based on p-stable distributions," in *Proceedings of the twentieth annual symposium on Computational geometry*, 2004, pp. 253–262.
- [15] M. Norouzi, A. Punjani, and D. J. Fleet, "Fast search in hamming space with multi-index hashing," in *Proceedings of CVPR'12*. IEEE, 2012, pp. 3108–3115.
- [16] A. Babenko and V. Lempitsky, "The inverted multi-index," *IEEE transactions on pattern analysis and machine intelligence*, vol. 37, no. 6, pp. 1247–1260, 2014.
- [17] P. Ram and A. G. Gray, "Maximum inner-product search using cone trees," in *Proceedings of the 18th ACM SIGKDD international conference on Knowledge discovery and data mining*. ACM, 2012, pp. 931–939.
- [18] F. P. Preparata and M. I. Shamos, *Computational geometry: an introduction*. Springer Science & Business Media, 2012.
- [19] A. Shrivastava and P. Li, "Improved asymmetric locality sensitive hashing (alsh) for maximum inner product search (mips)," *arXiv preprint arXiv:1410.5410*, 2014.
- [20] Y. Bachrach, Y. Finkelstein, R. Gilad-Bachrach, L. Katzir, N. Koenigstein, N. Nice, and U. Paquet, "Speeding up the xbox recommender system using a euclidean transformation for inner-product spaces," in *Proceedings of RecSys'14*. ACM, 2014, pp. 257–264.
- [21] B. Neyshabur and N. Srebro, "On symmetric and asym-

metric lshs for inner product search," in *Proceedings of ICML'15*, 2015, pp. 1926–1934.

[22] K. Zhou and H. Zha, "Learning binary codes for collaborative filtering," in *Proceedings of KDD'12*. ACM, 2012, pp. 498–506.

[23] N. Koenigstein, P. Ram, and Y. Shavitt, "Efficient retrieval of recommendations in a matrix factorization framework," in *Proceedings of CIKM'12*. ACM, 2012, pp. 535–544.

[24] R. Guo, S. Kumar, K. Choromanski, and D. Simcha, "Quantization based fast inner product search," in *Artificial Intelligence and Statistics*, 2016, pp. 482–490.

[25] S. Morozov and A. Babenko, "Non-metric similarity graphs for maximum inner product search," *Advances in Neural Information Processing Systems*, vol. 31, pp. 4721–4730, 2018.

[26] H. Zhang, F. Shen, W. Liu, X. He, H. Luan, and T.-S. Chua, "Discrete collaborative filtering," in *Proceedings of SIGIR'16*. ACM, 2016, pp. 325–334.

[27] D. Lian, R. Liu, Y. Ge, K. Zheng, X. Xie, and L. Cao, "Discrete content-aware matrix factorization," in *Proceedings of KDD'17*, 2017, pp. 325–334.

[28] D. Mazur, V. Egiazarian, S. Morozov, and A. Babenko, "Beyond vector spaces: compact data representation as differentiable weighted graphs," in *Proceedings of the 33rd International Conference on Neural Information Processing Systems*, 2019, pp. 6906–6916.

[29] D. Lian, X. Xie, E. Chen, and H. Xiong, "Product quantized collaborative filtering," *IEEE Transactions on Knowledge and Data Engineering*, vol. 33, no. 9, pp. 3284–3296, 2021.

[30] S. Tan, Z. Zhou, Z. Xu, and P. Li, "Fast item ranking under neural network based measures," in *Proceedings of the 13th International Conference on Web Search and Data Mining*, 2020, pp. 591–599.

[31] D. Lian, H. Wang, Z. Liu, J. Lian, E. Chen, and X. Xie, "Lightrec: A memory and search-efficient recommender system," in *Proceedings of The Web Conference 2020*, 2020, p. 695–705.

[32] D. Lian, Q. Liu, and E. Chen, "Personalized ranking with importance sampling," in *Proceedings of The Web Conference 2020*, 2020, pp. 1093–1103.

[33] D. Lian, Y. Wu, Y. Ge, X. Xie, and E. Chen, "Geography-aware sequential location recommendation," in *Proceedings of the 26th ACM SIGKDD international conference on knowledge discovery & data mining*, 2020, pp. 2009–2019.

[34] B. Jin, D. Lian, Z. Liu, Q. Liu, J. Ma, X. Xie, and E. Chen, "Sampling-decomposable generative adversarial recommender," *Advances in Neural Information Processing Systems*, vol. 33, pp. 22 629–22 639, 2020.

[35] S. Rendle and C. Freudenthaler, "Improving pairwise learning for item recommendation from implicit feedback," in *Proceedings of WSDM'14*. ACM, 2014, pp. 273–282.

[36] J. Weston, S. Bengio, and N. Usunier, "Large scale image annotation: learning to rank with joint word-image embeddings," *Machine learning*, vol. 81, no. 1, pp. 21–35, 2010.

[37] C.-K. Hsieh, L. Yang, Y. Cui, T.-Y. Lin, S. Belongie, and D. Estrin, "Collaborative metric learning," in *Proceedings of WWW'17*. International World Wide Web Conferences Steering Committee, 2017, pp. 193–201.

[38] W. Zhang, T. Chen, J. Wang, and Y. Yu, "Optimizing top-n collaborative filtering via dynamic negative item sampling," in *Proceedings of the 36th international ACM SIGIR conference on Research and development in information retrieval*. ACM, 2013, pp. 785–788.

[39] F. Morin and Y. Bengio, "Hierarchical probabilistic neural network language model," in *Aistats*, vol. 5. Citeseer, 2005, pp. 246–252.

[40] X. Li, T. Qin, J. Yang, and T.-Y. Liu, "Lightrnn: Memory and computation-efficient recurrent neural networks," in *Advances in Neural Information Processing Systems*, 2016, pp. 4385–4393.

[41] G. E. Hinton, "Training products of experts by minimizing contrastive divergence," *Neural computation*, vol. 14, no. 8, pp. 1771–1800, 2002.

[42] M. Gutmann and A. Hyvärinen, "Noise-contrastive estimation: A new estimation principle for unnormalized statistical models," in *Proceedings of the Thirteenth International Conference on Artificial Intelligence and Statistics*, 2010, pp. 297–304.

[43] I. Goodfellow, J. Pouget-Abadie, M. Mirza, B. Xu, D. Warde-Farley, S. Ozair, A. Courville, and Y. Bengio, "Generative adversarial nets," in *Advances in neural information processing systems*, 2014, pp. 2672–2680.

[44] J. Wang, L. Yu, W. Zhang, Y. Gong, Y. Xu, B. Wang, P. Zhang, and D. Zhang, "Irgan: A minimax game for unifying generative and discriminative information retrieval models," in *Proceedings of the 40th International ACM SIGIR conference on Research and Development in Information Retrieval*. ACM, 2017, pp. 515–524.

[45] I. J. Goodfellow, "On distinguishability criteria for estimating generative models," *arXiv preprint arXiv:1412.6515*, 2014.

[46] Z. Sun, Z.-H. Deng, J.-Y. Nie, and J. Tang, "Rotate: Knowledge graph embedding by relational rotation in complex space," *arXiv preprint arXiv:1902.10197*, 2019.

[47] G. Blanc and S. Rendle, "Adaptive sampled softmax with kernel based sampling," in *International Conference on Machine Learning*. PMLR, 2018, pp. 590–599.

[48] T. Zhang, "Statistical analysis of some multi-category large margin classification methods," *Journal of Machine Learning Research*, vol. 5, no. Oct, pp. 1225–1251, 2004.

[49] A. Tewari and P. L. Bartlett, "On the consistency of multiclass classification methods," *Journal of Machine Learning Research*, vol. 8, no. 5, 2007.

[50] M. Lapin, M. Hein, and B. Schiele, "Loss functions for top-k error: Analysis and insights," in *Proceedings of the IEEE conference on computer vision and pattern recognition*, 2016, pp. 1468–1477.

[51] M. Lapin, B. Schiele, and M. Hein, "Analysis and optimization of loss functions for multiclass, top-k, and multilabel classification," *IEEE transactions on pattern analysis and machine intelligence*, vol. 40, no. 7, pp. 1533–1554, 2017.

[52] F. Yang and S. Koyejo, "On the consistency of top-k surrogate losses," in *International Conference on Machine Learning*. PMLR, 2020, pp. 10 727–10 735.

[53] M. Wydmuch, K. Jasinska, M. Kuznetsov, R. Busa-Fekete, and K. Dembczynski, "A no-regret general-

ization of hierarchical softmax to extreme multi-label classification," *Advances in neural information processing systems*, vol. 31, 2018.

[54] J. Zhuo, Z. Xu, W. Dai, H. Zhu, H. Li, J. Xu, and K. Gai, "Learning optimal tree models under beam search," in *International Conference on Machine Learning*. PMLR, 2020, pp. 11650–11659.

[55] V. Koltchinskii and D. Panchenko, "Empirical margin distributions and bounding the generalization error of combined classifiers," *The Annals of Statistics*, vol. 30, no. 1, pp. 1–50, 2002.

[56] C. Cortes, M. Mohri, and A. Rostamizadeh, "Multi-class classification with maximum margin multiple kernel," in *International Conference on Machine Learning*. PMLR, 2013, pp. 46–54.

[57] Y. Lei, U. Dogan, D.-X. Zhou, and M. Kloft, "Data-dependent generalization bounds for multi-class classification," *IEEE Transactions on Information Theory*, vol. 65, no. 5, pp. 2995–3021, 2019.

[58] R. Babbar, I. Partalas, E. Gaussier, M.-R. Amini, and C. Amblard, "Learning taxonomy adaptation in large-scale classification," *The Journal of Machine Learning Research*, vol. 17, no. 1, pp. 3350–3386, 2016.

[59] A. Banerjee, X. Guo, and H. Wang, "On the optimality of conditional expectation as a bregman predictor," *IEEE Transactions on Information Theory*, vol. 51, no. 7, pp. 2664–2669, 2005.

[60] Y. Bengio and J.-S. Senécal, "Quick training of probabilistic neural nets by importance sampling," in *International Workshop on Artificial Intelligence and Statistics*. PMLR, 2003, pp. 17–24.

[61] Y. Bengio and J.-S. Senécal, "Adaptive importance sampling to accelerate training of a neural probabilistic language model," *IEEE Transactions on Neural Networks*, vol. 19, no. 4, pp. 713–722, 2008.

[62] A. S. Rawat, J. Chen, X. Y. Felix, A. T. Suresh, and S. Kumar, "Sampled softmax with random fourier features," in *NeurIPS*, 2019.

[63] B. Sarwar, G. Karypis, J. Konstan, and J. Riedl, "Item-based collaborative filtering recommendation algorithms," in *Proceedings of the 10th international conference on World Wide Web*, 2001, pp. 285–295.

[64] P. Covington, J. Adams, and E. Sargin, "Deep neural networks for youtube recommendations," in *Proceedings of the 10th ACM Conference on Recommender Systems*, New York, NY, USA, 2016.

[65] K. Jasinska, K. Dembczynski, R. Busa-Fekete, K. Pfannschmidt, T. Klerx, and E. Hullermeier, "Extreme f-measure maximization using sparse probability estimates," in *International conference on machine learning*. PMLR, 2016, pp. 1435–1444.

[66] D. P. Kingma and J. Ba, "Adam: A method for stochastic optimization," *arXiv preprint arXiv:1412.6980*, 2014.

[67] M. G. Hahn, "Probability in banach spaces: Isoperimetry and processes." 1994.

[68] L. Wan, M. Zeiler, S. Zhang, Y. Le Cun, and R. Fergus, "Regularization of neural networks using drop-connect," in *International conference on machine learning*. PMLR, 2013, pp. 1058–1066.

[69] S. Shalev-Shwartz and S. Ben-David, *Understanding machine learning: From theory to algorithms*. Cambridge university press, 2014.

APPENDIX A

NOTATIONS

Some important and common notations in this paper are summarized in Table 3.

TABLE 3
Some important and common notations in this paper.

Notations	Descriptions
\mathcal{U}, \mathcal{Y}	The user space and the item set.
\mathcal{T}, \mathcal{M}	The tree and the preference model.
$\mathcal{N}, \mathcal{N}^j$	The tree node set and the set of j -th level's nodes.
B, H	The branch number of \mathcal{T} and the tree height.
K	The length of historical interaction sequence.
L	The number of hidden layers in the neural network.
η_y	The conditional probability of the item y .
n, n_i^j	The tree node and the i -th node in the j -th level.
N_j	The number of nodes in level j .
N	The number of classes in multi-class classification.
$\rho^l(n)$	The ancestor of node n in level l .
π	The bijective mapping maps leaf nodes to items.
$\delta^j(y)$	The index of j -th ancestor of $\pi^{-1}(y)$ within its level.
$\mathcal{C}(n)$	The set of node n 's child nodes.
$\mathfrak{L}(n)$	The set of leaf nodes within the subtree rooted at n .
o_i^j, \hat{o}_i^j	The preference score and adjusted preference score for node n_i^j .
\mathcal{B}^j	The index set of selected nodes in layer j .
$z_i^j, \tilde{z}_i^j, \hat{z}_i^j$	The label, rectified label, and normalized rectified label for node n_i^j .
\mathcal{L}_j	The multi-class cross-entropy loss function of layer j .
$\tilde{\mathcal{L}}_j$	The modified loss function with rectified labels of layer j .
$\hat{\mathcal{L}}_j$	The loss function $\tilde{\mathcal{L}}_j$ incorporating sampled softmax.
M	The number of negative samples in sampled softmax.
\mathcal{I}_M^j	The set of indices of M negative nodes at layer j .
$\mathcal{R}_j, \tilde{\mathcal{R}}_j$	The conditional risk of loss \mathcal{L}_j and $\tilde{\mathcal{L}}_j$.
$\hat{\mathcal{R}}_m$	The empirical Rademacher complexity for a sample size m .
Q^j, P^j	The sampling distribution and softmax distribution in layer j .
q_i^j	The negative sampling probability for node n_i^j .
p_i^j	The softmax probability for node n_i^j based on the preference scores.

APPENDIX B

PROOFS OF LEMMA, PROPOSITION, AND THEOREM

B.1 Proof of Proposition 2

Proof. By taking $\psi(\mathbf{o}) = \sum_{n=1}^N x_n \log x_n$ and $g(\mathbf{o})_n = \exp o_n / \sum_{k=1}^N \exp o_k$, we have

$$\begin{aligned}
D_\psi & \left(\mathbf{e}^{(i)}(\mathbf{w}), g(\mathbf{o}) \right) \\
&= \psi \left(\mathbf{e}^{(i)}(\mathbf{w}) \right) - \psi \left(g(\mathbf{o}) \right) - \nabla \psi(g(\mathbf{o}))^T \left(\mathbf{e}^{(i)}(\mathbf{w}) - g(\mathbf{o}) \right) \\
&= w \log w - \sum_{n=1}^N g(\mathbf{o})_n \log g(\mathbf{o})_n \\
&\quad - \left\langle (\log g(\mathbf{o})_1 + 1, \dots, \log g(\mathbf{o})_i + 1, \dots, \log g(\mathbf{o})_n + 1), \right. \\
&\quad \quad \left. (-g(\mathbf{o})_1, \dots, w - g(\mathbf{o})_i, \dots, -g(\mathbf{o})_n) \right\rangle \\
&= w \log w - \sum_{n=1}^N g(\mathbf{o})_n \log g(\mathbf{o})_n \\
&\quad - \left(-\sum_{n=1}^N g(\mathbf{o})_n \log g(\mathbf{o})_n - 1 + w \log g(\mathbf{o})_i + w \right) \\
&= -w \log g(\mathbf{o})_i + w \log w + w - 1 = \tilde{\mathcal{L}}(\mathbf{e}^{(i)}(\mathbf{w}), \mathbf{o}).
\end{aligned}$$

B.2 Proof of Lemma 1

Proof. We complete the proof by contradiction. When $N_{j+1} \leq k$, $\arg\text{Topk} \mathbb{E}[\tilde{z}_i^{j+1}|u] = \{[N_{j+1}]\} = \mathcal{B}^{j+1}(u)$, so we only need to consider the case where $N_{j+1} > k$.

Denote $\arg\text{Topk} \mathbb{E}[\tilde{z}_i^{j+1}|u]$ as $\{\mathcal{D}_1^{j+1}, \mathcal{D}_2^{j+1}, \dots, \mathcal{D}_r^{j+1}\}_{i \in [N_{j+1}]}$ without loss of generality, where r is a natural number and each \mathcal{D}_i^{j+1} is a set of k elements. Suppose $\mathcal{B}^{j+1}(u) \notin \arg\text{Topk} \mathbb{E}[\tilde{z}_i^{j+1}|u]$, we can make the following derivation:

$$\begin{aligned}
& \mathcal{B}^{j+1}(u) \notin \arg\text{Topk} \mathbb{E}[\tilde{z}_i^{j+1}|u] \\
& \Rightarrow \mathcal{B}^{j+1}(u) \neq \mathcal{D}_i^{j+1} (1 \leq i \leq r) \\
& \Rightarrow \exists i_1, i_2 \in [N_{j+1}] \text{ s.t. } i_1 \in \mathcal{B}^{j+1}(u) \wedge i_1 \notin \mathcal{D}_i^{j+1} \\
& \quad \wedge i_2 \notin \mathcal{B}^{j+1}(u) \wedge i_2 \in \mathcal{D}_{i_0}^{j+1} (i_0 \in [r]) \\
& \Rightarrow \mathbb{E}[\tilde{z}_{i_1}^{j+1}|u] < \mathbb{E}[\tilde{z}_{i_2}^{j+1}|u] \wedge o_{i_1}^{j+1} \geq o_{i_2}^{j+1} \\
& \Rightarrow i_1 \in \tilde{\mathcal{B}}^{j+1}(u) \wedge i_2 \notin \tilde{\mathcal{B}}^{j+1}(u) \\
& \Rightarrow \delta(\rho^j(n_{i_1}^{j+1})) \in \mathcal{B}^j(u) \wedge \delta(\rho^j(n_{i_2}^{j+1})) \notin \mathcal{B}^j(u).
\end{aligned}$$

Let's denote $\mathcal{B}^j(u)$ as $\{s_1, s_2, \dots, s_k\}$, where the elements satisfy $o_{s_1}^j \geq o_{s_2}^j \geq \dots \geq o_{s_k}^j$. Notice that $R(\mathbf{o}^j, \mathbb{E}[\tilde{z}^j|u])$ and $\mathbb{E}[\tilde{z}_{s_i}^j|u] = \max_{n' \in \mathfrak{L}(n_{s_i}^j)} \eta_{\pi(n')}$, we have:

$$\max_{n' \in \mathfrak{L}(n_{s_1}^j)} \eta_{\pi(n')} \geq \max_{n' \in \mathfrak{L}(n_{s_2}^j)} \eta_{\pi(n')} \geq \dots \geq \max_{n' \in \mathfrak{L}(n_{s_k}^j)} \eta_{\pi(n')}. \quad (36)$$

For each node $n_{s_i}^j$, we then consider its node child $n_{c_i}^{j+1} \in \mathcal{C}(n_{s_i}^j)$ where $c_i = \underset{i \in \{\delta(n)|n \in \mathcal{C}(n_{s_i}^j)\}}{\text{argmax}} \mathbb{E}[\tilde{z}_i^{j+1}|u]$, and the following equation

$$\max_{n' \in \mathfrak{L}(n_{c_i}^{j+1})} \eta_{\pi(n')} = \max_{n' \in \mathfrak{L}(n_{s_i}^j)} \eta_{\pi(n')} \quad (37)$$

holds for $1 \leq i \leq k$. Combine the Eq. (36) and Eq. (37), we can get:

$$\max_{n' \in \mathfrak{L}(n_{c_1}^{j+1})} \eta_{\pi(n')} \geq \max_{n' \in \mathfrak{L}(n_{c_2}^{j+1})} \eta_{\pi(n')} \geq \dots \geq \max_{n' \in \mathfrak{L}(n_{c_k}^{j+1})} \eta_{\pi(n')}.$$

Then, for the $(j+1)$ -th layer, with $R(\mathbf{o}^{j+1}, \mathbb{E}[\tilde{z}^{j+1}|u])$ and $\mathbb{E}[\tilde{z}_{c_i}^{j+1}|u] = \max_{n' \in \mathfrak{L}(n_{c_i}^{j+1})} \eta_{\pi(n')}$, we have $o_{c_1}^{j+1} \geq o_{c_2}^{j+1} \geq \dots \geq o_{c_k}^{j+1}$, which means that the rank of $o_{c_k}^{j+1}$ in the components of \mathbf{o}^{j+1} is not lower than k . And because $i_1 \in \mathcal{B}^{j+1}(u)$, we can obtain the following results:

$$\begin{aligned}
o_{i_1}^{j+1} \geq o_{c_k}^{j+1} & \Rightarrow \mathbb{E}[\tilde{z}_{i_1}^{j+1}|u] \geq \mathbb{E}[\tilde{z}_{c_k}^{j+1}|u] \Rightarrow \mathbb{E}[\tilde{z}_{i_2}^{j+1}|u] > \mathbb{E}[\tilde{z}_{c_k}^{j+1}|u] \\
& \Rightarrow \max_{n' \in \mathfrak{L}(n_{i_2}^{j+1})} \eta_{\pi(n')} > \max_{n' \in \mathfrak{L}(n_{c_k}^{j+1})} \eta_{\pi(n')}.
\end{aligned} \quad (38)$$

Note that $i_\rho \triangleq \delta(\rho^j(n_{i_2}^{j+1})) \notin \mathcal{B}^j(u)$, $s_k \in \mathcal{B}^j(u)$, and $\mathcal{B}^j(u) \in \arg\text{Topk} \mathbb{E}[\tilde{z}_i^j|u]$, we can have $\mathbb{E}[\tilde{z}_{s_k}^j|u] \geq \mathbb{E}[\tilde{z}_{i_\rho}^j|u]$.

Therefore, we have

$$\max_{n' \in \mathfrak{L}(n_{s_k}^j)} \eta_{\pi(n')} \geq \max_{n' \in \mathfrak{L}(n_{i_\rho}^j)} \eta_{\pi(n')} \geq \max_{n' \in \mathfrak{L}(n_{i_2}^{j+1})} \eta_{\pi(n')}, \quad (39)$$

where the last inequality holds as the $\mathfrak{L}(n_{i_2}^{j+1}) \subseteq \mathfrak{L}(n_{i_\rho}^j)$. Combine the Eq. (37) and Eq. (39), we can get:

$$\max_{n' \in \mathfrak{L}(n_{c_k}^{j+1})} \eta_{\pi(n')} \geq \max_{n' \in \mathfrak{L}(n_{i_2}^{j+1})} \eta_{\pi(n')}. \quad (40)$$

Eq. (38) and Eq. (40) induces the contradiction, so the proposition holds. \square

B.3 Proof of Proposition 3

Proof. Let's consider the retrieval process along the tree for a given user u and a given beam size k .

Let $j^* = \operatorname{argmin}_{\{j: N_j > k\}} N_j$. When $1 \leq j \leq j^* - 1$, $\mathcal{B}^j(u) = \{[N_j]\} \in \operatorname{argTopk}_{i \in [N_j]} \mathbb{E}[\tilde{z}_i^j | u]$. When $j \geq j^*$, by recursively applying Lemma 1 from j^* to $H - 1$, we ultimately obtain $\mathcal{B}^H(u) \in \operatorname{argTopk}_{i \in [c(H)]} \mathbb{E}[\tilde{z}_i^H | u]$. Notice that $\mathbb{E}[\tilde{z}_i^H | u] = \eta_{\pi(n_i^H)}$, that is to say $\mathcal{B}^H(u) \in \operatorname{argTopk}_{i \in [N_H]} \eta_{\pi(n_i^H)}$, meaning the final retrieved item set $\hat{\mathcal{Y}} = \{\pi(n_i^H) | i \in \mathcal{B}^H(u)\} \in \operatorname{argTopk}_{y \in \mathcal{Y}} \eta_y(u)$.

The above analysis can be performed on any u and k , so the tree model is top- k retrieval Bayes optimal. \square

B.4 Proof of Proposition 4

Proof. We use induction to prove this proposition. Assume $\sum_{i=1}^{N_j} q_i^j = 1$, where q_i^j is the sampling probability of node n_i^j in the tree-based sampling, as presented in Eq. (24).

For the base case, when $j = 0$, the 0th layer contains only the root node n_1^0 , which is sampled with probability 1, and accordingly, the sum of sampling probabilities is exactly 1. Suppose the assumption holds for j , we now need to prove that it also holds for $j + 1$. For the layer $j + 1$, the sum of sampling probabilities for nodes within this layer is calculated as follows:

$$\begin{aligned} \sum_{i=1}^{N_{j+1}} q_i^{j+1} &= \sum_{i'=1}^{N_j} \sum_{i \in \{\delta(n) | n \in \mathcal{C}(n_{i'}^j)\}} q_i^{j+1} \\ &= \sum_{i'=1}^{N_j} \sum_{i \in \{\delta(n) | n \in \mathcal{C}(n_{i'}^j)\}} q_{i'}^j \tilde{q}_i^{j+1} \\ &= \sum_{i'=1}^{N_j} q_{i'}^j \sum_{i \in \{\delta(n) | n \in \mathcal{C}(n_{i'}^j)\}} \tilde{q}_i^{j+1} \\ &\stackrel{(a)}{=} \sum_{i'=1}^{N_j} q_{i'}^j = 1, \end{aligned} \quad (41)$$

where (a) holds as the sum of local softmax probabilities of all child nodes of one node is 1. \square

B.5 Proof of Theorem 3

Proof. We use induction to prove this theorem. Assume $q_i^j = \frac{\exp o_i^j}{\sum_{k=1}^{N_j} \exp o_k^j}$, where q_i^j denotes the sampling probability of node n_i^j in the tree-based sampling.

For the base case, when $j = 0$, the 0th layer contains only the root node n_1^0 , which is sampled with probability 1, equaling its softmax probability. Suppose the assumption holds for all nodes in layer j , we now need to prove that it also holds for all nodes in layer $j + 1$. For any n_i^j 's child node

n_c^{j+1} ($1 \leq c \leq N_{j+1}$) in layer $j + 1$, its sampling probability is calculated as follows:

$$\begin{aligned} q_c^{j+1} &= q_i^j \cdot \frac{\exp o_c^{j+1}}{\sum_{k \in \{\delta(n) | n \in \mathcal{C}(n_i^j)\}} \exp o_k^{j+1}} \\ &= \frac{\exp o_i^j}{\sum_{k=1}^{N_j} \exp o_k^j} \cdot \frac{\exp o_c^{j+1}}{\sum_{k \in \{\delta(n) | n \in \mathcal{C}(n_i^j)\}} \exp o_k^{j+1}} \end{aligned} \quad (42)$$

According to Eq. (25), and with the condition that the proportionality coefficients within the same layer are equal, we have

$$\begin{aligned} \sum_{k=1}^{N_j} \exp o_k^j &\propto \sum_{k=1}^{N_j} \sum_{k' \in \{\delta(n) | n \in \mathcal{C}(n_k^j)\}} \exp o_{k'}^{j+1} \\ &= \sum_{k=1}^{N_{j+1}} \exp o_k^{j+1}. \end{aligned} \quad (43)$$

Therefore, by substituting equations Eq. (25) and Eq. (43) into Eq. (42), we can obtain:

$$q_c^{j+1} = \frac{\exp o_c^{j+1}}{\sum_{k=1}^{N_{j+1}} \exp o_k^{j+1}}.$$

That is, when sampling to the $(j+1)$ -th layer in the tree-based sampling, the probability of sampling the corresponding node is equivalent to its softmax probability in layer $j+1$. As j increases, when reaching the last layer where the leaf nodes are located, this conclusion also holds. \square

B.6 Proof of Proposition 5

Proof. For node n_i^j , let the indices of its ancestors from the root to itself be denoted as $(\rho^0(i), \rho^1(i), \dots, \rho^{j-1}(i), \rho^j(i))$, where $\rho^l(i) = \delta(\rho^l(n_i^j))$ and $\rho^j(i)$ is exactly i . Denote the softmax probability $\frac{\exp o_i^j}{\sum_{k=1}^{N_j} \exp o_k^j}$ as p_i^j , then we have $\text{bias}_i^j = q_i^j - p_i^j$. Since the sampling probability is calculated as Eq. (24), we derive the following recurrence relation:

$$\begin{aligned} \text{bias}_i^j &= q_{\rho^{j-1}(i)}^{j-1} \tilde{q}_i^j - p_i^j \\ &= (q_{\rho^{j-1}(i)}^{j-1} - p_{\rho^{j-1}(i)}^{j-1}) \tilde{q}_i^j + p_{\rho^{j-1}(i)}^{j-1} \tilde{q}_i^j - p_i^j \\ &\stackrel{(a)}{=} (q_{\rho^{j-1}(i)}^{j-1} - p_{\rho^{j-1}(i)}^{j-1}) \tilde{q}_i^j \\ &\quad + \frac{\lambda_{\rho^{j-1}(i)}^{j-1} \exp o_i^j}{\sum_{k=1}^{N_j} \lambda_{\rho^{j-1}(k)}^{j-1} \exp o_k^j} - \frac{\exp o_i^j}{\sum_{k=1}^{N_j} \exp o_k^j} \\ &= \tilde{q}_i^j \text{bias}_{\rho^{j-1}(i)}^{j-1} + I(\rho^j(i), j), \end{aligned}$$

where (a) results from combining Eq. (27), Eq. (28), and analogous techniques used in Eq. (43), and $I(\rho^j(i), j) \triangleq \frac{\lambda_{\rho^{j-1}(i)}^{j-1} \exp o_{\rho^j(i)}^j}{\sum_{k=1}^{N_j} \lambda_{\rho^{j-1}(k)}^{j-1} \exp o_k^j} - \frac{\exp o_{\rho^j(i)}^j}{\sum_{k=1}^{N_j} \exp o_k^j}$.

Notably, $\text{bias}_1^0 = 0$ and $\text{bias}_i^1 = 0$ for $i \in [N_1]$. For $j \geq 2$, we obtain:

$$\text{bias}_i^j = \sum_{k=2}^{j-1} I(\rho^k(i), k) \cdot \prod_{t=k+1}^j \tilde{q}_{\rho^t(i)}^t + I(\rho^j(i), j).$$

Given that $\lambda_i^j \in (1 - \varepsilon, 1)$ holds for any $i \in N_j$ and $j \in [H]$, it follows that

$$|I(\rho^k(i), k)| \leq \frac{\varepsilon}{1 - \varepsilon} p_{\rho^k(i)}^k \leq \frac{\varepsilon}{1 - \varepsilon}.$$

Thus, we conclude

$$|\text{bias}_i^j| \leq \frac{(j-1)\varepsilon}{1 - \varepsilon}.$$

By applying the Eq. (45), we can get:

$$\begin{aligned} \widehat{\mathcal{R}}_m(\mathcal{M}) &= \mathbb{E}_\sigma \left[\sup_{f \in \mathcal{M}} \frac{1}{m} \sum_{i=1}^m \sigma_i f(u_i, n_i) \right] \\ &= \mathbb{E}_\sigma \left[\sup_{\mathbf{z}, \mathbf{w}_n, \{\mathbf{W}_k\}_{k=1}^L} \frac{1}{m} \sum_{i=1}^m \sigma_i \left\langle \mathbf{W}_L, \phi_{L-1} \circ \right. \right. \\ &\quad \left. \phi_{L-2} \circ \cdots \circ \phi_1 \left(\mathbf{z}_1^{(u_i)}; \mathbf{z}_2^{(u_i)}; \dots; \mathbf{z}_{K'}^{(u_i)}; \mathbf{w}_{n_i} \right) \right\rangle \Big] \\ &\stackrel{(a)}{\leq} \|\mathbf{W}_L\|_1 \mathbb{E}_\sigma \left[\sup_{\substack{s \in \{-1, 1\}, j \in [d_{L-1}] \\ \mathbf{z}, \mathbf{w}_n, \{\mathbf{W}_k\}_{k=1}^{L-1}}} \frac{1}{m} \sum_{i=1}^m s \sigma_i \left\langle \mathbf{e}_j, \phi_{L-1} \circ \right. \right. \\ &\quad \left. \phi_{L-2} \circ \cdots \circ \phi_1 \left(\mathbf{z}_1^{(u_i)}; \mathbf{z}_2^{(u_i)}; \dots; \mathbf{z}_{K'}^{(u_i)}; \mathbf{w}_{n_i} \right) \right\rangle \Big] \\ &\stackrel{(b)}{\leq} c_\phi \|\mathbf{W}_L\|_1 \mathbb{E}_\sigma \left[\sup_{\substack{s \in \{-1, 1\}, j \in [d_{L-1}] \\ \mathbf{z}, \mathbf{w}_n, \{\mathbf{W}_k\}_{k=1}^{L-1}}} \frac{1}{m} \sum_{i=1}^m s \sigma_i \left\langle \mathbf{e}_j, \mathbf{W}_{L-1} \circ \right. \right. \\ &\quad \left. \phi_{L-2} \circ \cdots \circ \phi_1 \left(\mathbf{z}_1^{(u_i)}; \mathbf{z}_2^{(u_i)}; \dots; \mathbf{z}_{K'}^{(u_i)}; \mathbf{w}_{n_i} \right) \right\rangle \Big] \\ &\stackrel{(c)}{\leq} c_\phi \|\mathbf{W}_L\|_1 \|\mathbf{W}_{L-2}\|_1 \mathbb{E}_\sigma \left[\sup_{\substack{s \in \{-1, 1\}, j \in [d_{L-2}] \\ \mathbf{z}, \mathbf{w}_n, \{\mathbf{W}_k\}_{k=1}^{L-1}}} \frac{1}{m} \sum_{i=1}^m s \sigma_i \right. \\ &\quad \left. \left\langle \mathbf{e}_j, \phi_{L-2} \circ \cdots \circ \phi_1 \left(\mathbf{z}_1^{(u_i)}; \mathbf{z}_2^{(u_i)}; \dots; \mathbf{z}_{K'}^{(u_i)}; \mathbf{w}_{n_i} \right) \right\rangle \Big] \right. \\ &\stackrel{(d)}{\leq} 2c_\phi^{L-1} \prod_{k=1}^L \|\mathbf{W}_k\|_1 \mathbb{E}_\sigma \left[\sup_{\substack{\mathbf{z}, \mathbf{w}_n, \\ j \in [(K'+1)d]}} \frac{1}{m} \sum_{i=1}^m \sigma_i \left\langle \mathbf{e}_j, \right. \right. \\ &\quad \left. \left. \left(\mathbf{z}_1^{(u_i)}; \mathbf{z}_2^{(u_i)}; \dots; \mathbf{z}_{K'}^{(u_i)}; \mathbf{w}_{n_i} \right) \right\rangle \right] \\ &\leq 2c_\phi^{L-1} \prod_{k=1}^L \|\mathbf{W}_k\|_1 \left(\underbrace{\mathbb{E}_\sigma \left[\sup_{j \in [d], \mathbf{w}_n} \frac{1}{m} \sum_{i=1}^m \sigma_i \langle \mathbf{e}_j, \mathbf{w}_{n_i} \rangle \right]}_{I_1} \right. \\ &\quad \left. + \sum_{t=1}^{K'} \underbrace{\mathbb{E}_\sigma \left[\sup_{j \in [d], \mathbf{z}_t} \frac{1}{m} \sum_{i=1}^m \sigma_i \langle \mathbf{e}_j, \mathbf{z}_t^{(u_i)} \rangle \right]}_{I_2} \right) \end{aligned} \quad (46)$$

Proof. For $\forall i \in [N_j]$, $|o_i^j| \leq B_o$, then we can obtain:

$$p_i^j = \frac{\exp o_i^j}{\sum_{k=1}^{N_j} \exp o_k^j} \geq \frac{\exp(-B_o)}{N_j \exp B_o} = \frac{1}{N_j \exp 2B_o}.$$

Then, we have

$$\begin{aligned} D_{KL}(Q^j || P^j) &= \sum_{i=1}^{N_j} q_i^j \log \frac{q_i^j}{p_i^j} \\ &= \sum_{i=1}^{N_j} q_i^j \log \left(1 + \frac{\text{bias}_i^j}{p_i^j} \right) \\ &\leq \sum_{i=1}^{N_j} q_i^j \log \left(1 + \text{bias}_i^j N_j e^{2B_o} \right) \quad (44) \\ &\leq \sum_{i=1}^{N_j} q_i^j \log \left(1 + B_\varepsilon^j N_j e^{2B_o} \right) \\ &= \log \left(1 + B_\varepsilon^j N_j e^{2B_o} \right), \end{aligned}$$

where $B_\varepsilon^j \triangleq \frac{(j-1)\varepsilon}{1 - \varepsilon}$ and $\text{bias}_i^j \leq B_\varepsilon^j$ as presented in Proposition 5. \square

B.8 Proof of Lemma 2

Proof. For any vectors $\mathbf{v}, \mathbf{u}_i \in \mathbb{R}^d$, $\|\mathbf{v}\|_1 \leq B_v$, notice the following inequality:

$$\sup_{\mathbf{v}} \sum_i \mathbf{v}^\top \mathbf{u}_i \leq B_v \max_{j \in [d]} \left| \sum_i \mathbf{e}_j \mathbf{u}_i \right| \leq \sum_i B_v \max_{\substack{j \in [d] \\ s \in \{-1, 1\}}} s \mathbf{e}_j \mathbf{u}_i. \quad (45)$$

where (a) use Eq. (45) as $\mathbf{W}_L \in \mathbb{R}^{1 \times d_{L-1}}$ is actually a vector; (b) holds since σ is applied element wise, we can bring \mathbf{e}_j^T inside the function and the use of contraction inequality [67]; (c) use Eq. (45) again as $\mathbf{e}_j^T \mathbf{W}_{L-1}$ is still a vector; (d) holds by applying Eq. (45) recursively and utilizing the fact that $\widehat{\mathcal{R}}_m(\mathcal{F} \cup -\mathcal{F}) \leq 2\widehat{\mathcal{R}}_m(\mathcal{F})$.

As the term I_1 , using Cauchy-Schwartz inequality and Jensen inequality, we have:

$$\begin{aligned} I_1 &\leq \frac{1}{m} \mathbb{E}_\sigma \left[\left\| \sum_{i=1}^m \sigma_i \mathbf{w}_{n_i} \right\|_2 \right] \leq \frac{1}{m} \left(\mathbb{E}_\sigma \left[\left\| \sum_{i=1}^m \sigma_i \mathbf{w}_{n_i} \right\|_2^2 \right] \right)^{1/2} \\ &= \frac{1}{m} \left(\sum_{i=1}^m \|\mathbf{w}_{n_i}\|^2 \right)^{1/2} \leq \frac{B_0}{\sqrt{m}}. \end{aligned} \quad (47)$$

As the term I_2 , we have:

$$\begin{aligned}
I_2 &= \frac{1}{m} \mathbb{E}_\sigma \left[\sup_{j \in [d], \mathbf{w}} \sum_{i=1}^m \sigma_i \left\langle \mathbf{e}_j, \sum_{k \in T_t} w_k^{(u_i)} \mathbf{a}_k^{(u_i)} \right\rangle \right] \\
&\leq \frac{1}{m} \sum_{k \in T_t} \mathbb{E}_\sigma \left[\sup_{j \in [d], \mathbf{w}} \sum_{i=1}^m \sigma_i \left\langle \mathbf{e}_j, w_k^{(u_i)} \mathbf{a}_k^{(u_i)} \right\rangle \right] \\
&= \frac{1}{m} \sum_{k \in T_t} \mathbb{E}_\sigma \left[\sup_{j \in [d], \mathbf{w}} \sum_{i=1}^m \sigma_i \phi \left(\mathbf{W}_w^{(2)} \phi \left(\mathbf{W}_w^{(1)} \right. \right. \right. \\
&\quad \left. \left. \left. \left[\mathbf{a}_k^{(u_i)}; \mathbf{a}_k^{(u_i)} \odot \mathbf{w}_{n_i}; \mathbf{w}_{n_i} \right] \right) \right) \left\langle \mathbf{e}_j, \mathbf{a}_k^{(u_i)} \right\rangle \right] \\
&\leq \frac{1}{m} c_\phi^2 \left\| \mathbf{W}_w^{(1)} \right\|_1 \left\| \mathbf{W}_w^{(2)} \right\|_1 \sum_{k \in T_t} \mathbb{E}_\sigma \left[\sup_{\substack{\mathbf{w}, j \in [d] \\ j' \in [3d]}} \sum_{i=1}^m \sigma_i \right. \\
&\quad \left. \left\langle \mathbf{e}_{j'}, \left[\mathbf{a}_k^{(u_i)}; \mathbf{a}_k^{(u_i)} \odot \mathbf{w}_{n_i}; \mathbf{w}_{n_i} \right] \right\rangle \left\langle \mathbf{e}_j, \mathbf{a}_k^{(u_i)} \right\rangle \right]. \quad (48)
\end{aligned}$$

Furthermore, we can get

$$\begin{aligned}
&\mathbb{E}_\sigma \left[\sup_{\substack{\mathbf{w}, j \in [d] \\ j' \in [3d]}} \sum_{i=1}^m \sigma_i \left\langle \mathbf{e}_{j'}, \left[\mathbf{a}_k^{(u_i)}; \mathbf{a}_k^{(u_i)} \odot \mathbf{w}_{n_i}; \mathbf{w}_{n_i} \right] \right\rangle \left\langle \mathbf{e}_j, \mathbf{a}_k^{(u_i)} \right\rangle \right] \\
&\leq \mathbb{E}_\sigma \left[\sup_{j \in [d], j' \in [d]} \sum_{i=1}^m \sigma_i \left\langle \mathbf{e}_{j'}, \mathbf{a}_k^{(u_i)} \right\rangle \left\langle \mathbf{e}_j, \mathbf{a}_k^{(u_i)} \right\rangle \right] \\
&\quad + \mathbb{E}_\sigma \left[\sup_{j \in [d], j' \in [d], \mathbf{w}} \sum_{i=1}^m \sigma_i \left\langle \mathbf{e}_{j'}, \mathbf{a}_k^{(u_i)} \odot \mathbf{w}_{n_i} \right\rangle \left\langle \mathbf{e}_j, \mathbf{a}_k^{(u_i)} \right\rangle \right] \\
&\quad + \mathbb{E}_\sigma \left[\sup_{j \in [d], j' \in [d], \mathbf{w}} \sum_{i=1}^m \sigma_i \left\langle \mathbf{e}_{j'}, \mathbf{w}_{n_i} \right\rangle \left\langle \mathbf{e}_j, \mathbf{a}_k^{(u_i)} \right\rangle \right] \\
&= I_3 + I_4 + I_5. \quad (49)
\end{aligned}$$

As the term I_3 , notice that

$$\begin{aligned}
\sum_{i=1}^m \sigma_i \left\langle \mathbf{e}_{j'}, \mathbf{a}_k^{(u_i)} \right\rangle \left\langle \mathbf{e}_j, \mathbf{a}_k^{(u_i)} \right\rangle &= \sum_{i=1}^m \sigma_i \mathbf{e}_{j'}^\top \mathbf{P}_a^{(u_i)} \mathbf{e}_j \\
&= \sum_{i=1}^m \sigma_i \text{Tr} \left(\mathbf{e}_j \mathbf{e}_{j'}^\top \mathbf{P}_a^{(u_i)} \right) = \text{Tr} \left(\mathbf{e}_j \mathbf{e}_{j'}^\top \left(\sum_{i=1}^m \sigma_i \mathbf{P}_a^{(u_i)} \right) \right) \\
&= \left\langle \mathbf{e}_j \mathbf{e}_{j'}^\top, \sum_{i=1}^m \sigma_i \mathbf{P}_a^{(u_i)} \right\rangle_F,
\end{aligned}$$

where $\mathbf{P}_a^{(u_i)} = \mathbf{a}_k^{(u_i)} \mathbf{a}_k^{(u_i)^\top}$. Then, we can get

$$\begin{aligned}
I_3 &= \mathbb{E}_\sigma \left[\sup_{j \in [d], j' \in [d]} \sum_{i=1}^m \sigma_i \left\langle \mathbf{e}_{j'}, \mathbf{a}_k^{(u_i)} \right\rangle \left\langle \mathbf{e}_j, \mathbf{a}_k^{(u_i)} \right\rangle \right] \\
&= \mathbb{E}_\sigma \left[\sup_{j \in [d], j' \in [d]} \left\langle \mathbf{e}_j \mathbf{e}_{j'}^\top, \sum_{i=1}^m \sigma_i \mathbf{P}_a^{(u_i)} \right\rangle_F \right] \\
&\leq \mathbb{E}_\sigma \left[\left\| \sum_{i=1}^m \sigma_i \mathbf{P}_a^{(u_i)} \right\|_F \right] = \sqrt{\sum_{i=1}^m \left\| \mathbf{P}_a^{(u_i)} \right\|_F^2} \leq \sqrt{m B_a^4}. \quad (50)
\end{aligned}$$

As the term I_4 , use the same analysis technique as for I_3 , we can get

$$\begin{aligned}
I_4 &= \mathbb{E}_\sigma \left[\sup_{j \in [d], j' \in [d], \mathbf{w}} \sum_{i=1}^m \sigma_i \left\langle \mathbf{e}_{j'}, \mathbf{a}_k^{(u_i)} \odot \mathbf{w}_{n_i} \right\rangle \left\langle \mathbf{e}_j, \mathbf{a}_k^{(u_i)} \right\rangle \right] \\
&= \mathbb{E}_\sigma \left[\sup_{j \in [d], j' \in [d], \mathbf{w}} \sum_{i=1}^m \sigma_i \left\langle \mathbf{e}_{j'} \odot \mathbf{w}_{n_i}, \mathbf{a}_k^{(u_i)} \right\rangle \left\langle \mathbf{e}_j, \mathbf{a}_k^{(u_i)} \right\rangle \right] \\
&= \mathbb{E}_\sigma \left[\sup_{j \in [d], j' \in [d], \mathbf{w}} \sum_{i=1}^m \sigma_i \left\langle \mathbf{e}_j \mathbf{e}_{j'}^\top \odot \mathbf{w}_{n_i}^\top, \mathbf{P}_a^{(u_i)} \right\rangle_F \right] \\
&= \mathbb{E}_\sigma \left[\sup_{j \in [d], j' \in [d], \mathbf{w}} \sum_{n \in \mathcal{N}} \sum_{i: n_i=n} \sigma_i \left\langle \mathbf{e}_j \mathbf{e}_{j'}^\top \odot \mathbf{w}_n^\top, \mathbf{P}_a^{(u_i)} \right\rangle_F \right] \\
&\leq \sum_{n \in \mathcal{N}} \mathbb{E}_\sigma \left[\sup_{j \in [d], j' \in [d]} \left\langle \mathbf{e}_j \mathbf{e}_{j'}^\top \odot \mathbf{w}_n^\top, \sum_{i: n_i=n} \sigma_i \mathbf{P}_a^{(u_i)} \right\rangle_F \right] \\
&\leq B_0 \sum_{n \in \mathcal{N}} \mathbb{E}_\sigma \left[\left\| \sum_{i: n_i=n} \sigma_i \mathbf{P}_a^{(u_i)} \right\|_F \right] \\
&\leq B_0 B_a^2 \sum_{n \in \mathcal{N}} \sqrt{|\{i : n_i = n\}|} \leq B_0 B_a^2 \sqrt{\frac{2B-1}{B-1} |\mathcal{Y}| m}, \quad (51)
\end{aligned}$$

where the last inequality holds as $\sum_{n \in \mathcal{N}} |\{i : n_i = n\}| = m$, $|\mathcal{N}| = \sum_{j=0}^{\lceil \log_2 |\mathcal{Y}| \rceil - 1} B^j + |\mathcal{Y}| \leq \frac{2B-1}{B-1} |\mathcal{Y}|$ for the B -ary tree, and use the Cauchy-Schwartz inequality.

As the term I_5 , use the same technique as for I_4 , we have

$$\begin{aligned}
I_5 &= \mathbb{E}_\sigma \left[\sup_{j \in [d], j' \in [d], \mathbf{w}} \sum_{i=1}^m \sigma_i \left\langle \mathbf{e}_{j'}, \mathbf{w}_{n_i} \right\rangle \left\langle \mathbf{e}_j, \mathbf{a}_k^{(u_i)} \right\rangle \right] \\
&= \mathbb{E}_\sigma \left[\sup_{j \in [d], j' \in [d], \mathbf{w}} \sum_{n \in \mathcal{N}} \sum_{i: n_i=n} \sigma_i \left\langle \mathbf{e}_{j'}, \mathbf{w}_{n_i} \right\rangle \left\langle \mathbf{e}_j, \mathbf{a}_k^{(u_i)} \right\rangle \right] \\
&\leq \sum_{n \in \mathcal{N}} \mathbb{E}_\sigma \left[\sup_{j \in [d], j' \in [d]} \left\langle \mathbf{e}_{j'}, \mathbf{w}_n \right\rangle \left\langle \mathbf{e}_j, \sum_{i: n_i=n} \sigma_i \mathbf{a}_k^{(u_i)} \right\rangle \right] \\
&\leq B_0 \sum_{n \in \mathcal{N}} \mathbb{E}_\sigma \left[\left\| \sum_{i: n_i=n} \sigma_i \mathbf{a}_k^{(u_i)} \right\|_2 \right] \leq B_0 B_a \sqrt{\frac{2B-1}{B-1} |\mathcal{Y}| m}. \quad (52)
\end{aligned}$$

Combine equations Eq. (46)~Eq. (52), and notice the fact that $\sum_{t=1}^{K'} T_t = K$, we have

$$\begin{aligned}
\widehat{\mathcal{R}}_m(\mathcal{M}) &= \mathbb{E}_\sigma \left[\sup_{f \in \mathcal{M}} \frac{1}{m} \sum_{i=1}^m \sigma_i f(u_i, n_i) \right] \\
&\leq 2c_\phi^{L-1} \prod_{k=1}^L \left\| \mathbf{W}_k \right\|_1 \left[\frac{B_0}{\sqrt{m}} + c_\phi^2 \left\| \mathbf{W}_w^{(1)} \right\|_1 \left\| \mathbf{W}_w^{(2)} \right\|_1 K \cdot \right. \\
&\quad \left. \left(\frac{B_a^2}{\sqrt{m}} + \frac{B_0 B_a^2}{\sqrt{m}} \sqrt{\frac{2B-1}{B-1} |\mathcal{Y}|} + \frac{B_0 B_a}{\sqrt{m}} \sqrt{\frac{2B-1}{B-1} |\mathcal{Y}|} \right) \right] \\
&\leq \frac{2c_\phi^{L-1} B_1^L (B_0 + K B_{w_1} + K B_{w_2} \tau)}{\sqrt{m}},
\end{aligned}$$

where $B_{w_1} = c_\phi^2 B_2^2 B_a^2$, $B_{w_2} = c_\phi^2 B_0 B_2^2 (B_a^2 + B_a)$, $\tau = \sqrt{(2B-1)|\mathcal{Y}|}/\sqrt{B-1}$. \square

B.9 Proof of Lemma 3

Proof. Given the sample set $S = \{u_i, y_i\}_{i=1}^m$, we consider the loss function space $\mathcal{F}_\ell^j = \{(u, y) \rightarrow f_\ell^j(u, y)\}$, where

function $f_\ell^j(u, y) = \tilde{\mathcal{L}}_j(u, y) = -\tilde{z}_{\delta^j(y)}^j \log \frac{\exp o_{\delta^j(y)}^j(u)}{\sum_{k=1}^{N_j} \exp o_k^j(u)}$ and $o_k^j(u) = f_{\text{DIN}}(u, n_k^j)$. Due to $|f_{\text{DIN}}| \leq B_{\mathcal{M}}$, we can get $|f_\ell^j| \leq 2B_{\mathcal{M}} + \log N_j$. Then, by the Lemma 5, we have:

$$\begin{aligned} \mathbb{E}_{(u,y) \sim \mathbb{P}} [\tilde{\mathcal{L}}_j(u, y)] &\leq \frac{1}{m} \sum_{i=1}^m \tilde{\mathcal{L}}_j(u_i, y_i) + 2\hat{\mathcal{R}}_m(\mathcal{F}_\ell^j, S) \\ &\quad + (4 \log N_j + 8B_{\mathcal{M}}) \sqrt{\frac{2 \log (4/\delta)}{m}}. \end{aligned} \quad (53)$$

For the empirical Rachemader complexity of \mathcal{F}_ℓ^j , we have

$$\begin{aligned} \hat{\mathcal{R}}_m(\mathcal{F}_\ell^j, S) &= \mathbb{E}_\sigma \left[\sup_{f_\ell^j \in \mathcal{F}_\ell^j} \frac{1}{m} \sum_{i=1}^m \sigma_i f_\ell^j(u_i, y_i) \right] \\ &= \mathbb{E}_\sigma \left[\sup_{\substack{f_{\text{DIN}} \in \mathcal{M} \\ \tilde{z} \in \{0,1\}}} \frac{1}{m} \sum_{i=1}^m \sigma_i \tilde{z}_{\delta^j(y_i)}^j \log \frac{\sum_{k=1}^{N_j} \exp o_k^j(u_i)}{\exp o_{\delta^j(y_i)}^j(u_i)} \right] \\ &= \mathbb{E}_\sigma \left[\sup_{\substack{f_{\text{DIN}} \in \mathcal{M} \\ z' \triangleq 2\tilde{z}-1 \in \{-1,1\}}} \frac{1}{m} \sum_{i=1}^m \sigma_i \frac{z'+1}{2} \log \frac{\sum_{k=1}^{N_j} \exp o_k^j(u_i)}{\exp o_{\delta^j(y_i)}^j(u_i)} \right] \\ &\leq \mathbb{E}_\sigma \left[\sup_{f_{\text{DIN}} \in \mathcal{M}} \frac{1}{m} \sum_{i=1}^m \sigma_i * -\log \frac{\exp o_{\delta^j(y_i)}^j(u_i)}{\sum_{k=1}^{N_j} \exp o_k^j(u_i)} \right] \\ &= \hat{\mathcal{R}}_m(\ell \circ \mathcal{M}, S), \end{aligned} \quad (54)$$

where the last equality holds because

$$-\log \frac{\exp o_{\delta^j(y_i)}^j(u_i)}{\sum_{k=1}^{N_j} \exp o_k^j(u_i)} = -\sum_{n=1}^{N_j} \mathbb{I}(n = \delta^j(y_i)) \cdot \log \frac{\exp o_n^j(u_i)}{\sum_{k=1}^{N_j} \exp o_k^j(u_i)}$$

is a composition of logistic loss $\ell_y(\mathbf{o}) = -\sum_i y_i \log \frac{\exp o_i}{\sum_j \exp o_j}$ and f_{DIN} . Since the partial derivative of $\ell_y(\mathbf{o})$ w.r.t. each component is bounded by 1, the logistic loss function ℓ is 1-Lipschitz [68]. For the j -th layer, where the number of classes is N_j , by Lemma 6, we have

$$\hat{\mathcal{R}}_m(\ell \circ \mathcal{M}, S) \leq 2N_j \hat{\mathcal{R}}_m(\mathcal{M}, S). \quad (55)$$

Combine the Eq. (53), Eq. (B.9) and Eq. (55), and utilize the Lemma 2, we can obtain the desired result. \square

B.10 Proof of Lemma 4

Proof. The i -th node is positive among N_j nodes in the j -th layer, and the sampling distribution is Q^j , with the sampling probability $q_{i'}^j$ for node $n_{i'}^j$. Therefore, according to Eq. (21), for $i' \in \mathcal{I}_M^j \cup \{i\}$, the adjusted logit is calculated as follows:

$$\hat{o}_{i'}^j = \begin{cases} o_i^j - \ln(Mq_{i'}^j) & \text{if } i' \neq i \\ o_i^j - \ln(1) & \text{if } i' = i \end{cases} \quad (56)$$

Then, we can have:

$$\begin{aligned} &\ell_{\text{softmax}}^j(u, y) - \mathbb{E}_{\mathcal{I}_M^j} [\ell_{\text{sampled-softmax}}^j(u, y, \mathcal{I}_M^j)] \\ &= -\log \frac{\exp o_i^j}{\sum_{k=1}^{N_j} \exp o_k^j} - \mathbb{E}_{\mathcal{I}_M^j} \left[-\log \frac{\exp \hat{o}_i^j}{\sum_{i' \in \mathcal{I}_M^j \cup \{i\}} \exp \hat{o}_{i'}^j} \right] \\ &= \mathbb{E}_{\mathcal{I}_M^j} \left[\log \left(\sum_{k=1}^{N_j} \exp o_k^j \right) - \log \left(\exp o_i^j + \sum_{i' \in \mathcal{I}_M^j} \frac{\exp o_{i'}^j}{Mq_{i'}^j} \right) \right] \\ &= \mathbb{E}_{\mathcal{I}_M^j} \left[-\log \left(p_i^j + \frac{1}{M} \sum_{i' \in \mathcal{I}_M^j} \frac{p_{i'}^j}{q_{i'}^j} \right) \right] \\ &= \mathbb{E}_{\mathcal{I}_M^j} \left[\log \frac{M}{\sum_{i' \in \mathcal{I}_M^j} \left(\frac{q_{i'}^j}{p_{i'}^j + p_i^j q_{i'}^j} \right)^{-1}} \right] \\ &\stackrel{(a)}{\leq} \mathbb{E}_{\mathcal{I}_M^j} \left[\log \left(\prod_{i' \in \mathcal{I}_M^j} \frac{q_{i'}^j}{p_{i'}^j + p_i^j q_{i'}^j} \right)^{\frac{1}{M}} \right] \\ &= \frac{1}{M} \sum_{i' \in \mathcal{I}_M^j} \mathbb{E}_{i' \sim Q^j} \left[\log \frac{q_{i'}^j}{p_{i'}^j + p_i^j q_{i'}^j} \right] \\ &\leq \frac{1}{M} \sum_{i' \in \mathcal{I}_M^j} \mathbb{E}_{i' \sim Q^j} \left[\log \left(\frac{q_{i'}^j}{p_{i'}^j} \right) \right] = D_{\text{KL}}(Q^j \| P^j), \end{aligned}$$

where (a) uses Harmonic-Geometric inequality. \square

B.11 Proof of Theorem 4

Proof. By Lemma 4, we have

$$\begin{aligned} &\mathbb{E}_{(u,y) \sim \mathbb{P}} [\tilde{\mathcal{L}}_j(u, y)] - \mathbb{E}_{(u,y), \mathcal{I}_M^j} [\hat{\mathcal{L}}_j(u, y)] \\ &\leq \mathbb{E}_{(u,y) \sim \mathbb{P}} [D_{\text{KL}}(Q^j \| P^j)], \end{aligned} \quad (57)$$

For convenience, we omit the subscripts of the expectations and use \mathbb{E} to denote the expectation taken over u , y , and \mathcal{I}_M^j . From Lemma 5, we have:

$$\begin{aligned} \mathbb{E} [\hat{\mathcal{L}}_j(u, y)] &\leq \frac{1}{m} \sum_{i=1}^m \hat{\mathcal{L}}_j(u_i, y_i) + 2\hat{\mathcal{R}}_m(\hat{\mathcal{F}}_\ell^j, S) \\ &\quad + (4 \log N_j + 8B_{\mathcal{M}}) \sqrt{\frac{2 \log (4/\delta)}{m}}. \end{aligned} \quad (58)$$

where

$$\begin{aligned} \hat{\mathcal{R}}_m(\hat{\mathcal{F}}_\ell^j, S) &= \mathbb{E}_\sigma \left[\sup_{\hat{f}_\ell^j \in \hat{\mathcal{F}}_\ell^j} \frac{1}{m} \sum_{i=1}^m \sigma_i \hat{f}_\ell^j(u_i, y_i) \right] \\ &= \mathbb{E}_\sigma \left[\sup_{\substack{f_{\text{DIN}} \in \mathcal{M} \\ \tilde{z} \in \{0,1\}}} \frac{1}{m} \sum_{i=1}^m \sigma_i \tilde{z}_{\delta^j(y_i)}^j \log \frac{\sum_{k \in \mathcal{I}_M^j \cup \{\delta^j(y_i)\}} \exp o_k^j(u_i)}{\exp o_{\delta^j(y_i)}^j(u_i)} \right]. \end{aligned} \quad (59)$$

Using the same analysis method with Eq. (B.9) and Eq. (55) in the proof of Lemma 3, we can get

$$\hat{\mathcal{R}}_m(\hat{\mathcal{F}}_\ell^j, S) \leq 2(|\mathcal{I}_M^j| + 1) \hat{\mathcal{R}}_m(\mathcal{M}, S) \leq 2N_j \hat{\mathcal{R}}_m(\mathcal{M}, S). \quad (60)$$

Combine above equations Eq. (57)~Eq. (60), and Lemma 2, and aggregate from 1st layer to H -th layer, we can get the desired result. \square

APPENDIX C

AUXILIARY LEMMAS

Lemma 5 (Theorem 26.5(2) of [69]). *If the magnitude of loss function l is bounded above by c , with probability greater than $1 - \delta$ for all $h \in \mathcal{H}$, we have*

$$\begin{aligned} \mathbb{E}_{(x,y) \sim \mathcal{D}}[\ell(h(x), y)] &\leq \frac{1}{m} \sum_{i=1}^m \ell(h(x_i), y_i) \\ &\quad + 2\hat{\mathcal{R}}_m(\ell \circ \mathcal{H}, S) + 4c\sqrt{\frac{2 \ln(4/\delta)}{m}} \end{aligned}$$

where $\ell \circ \mathcal{H} = \{\ell(h(x), y) \mid (x, y) \in \mathcal{X} \times \mathcal{Y}, h \in \mathcal{H}\}$.

Lemma 6 (Lemma 2 of [68]). *Let \mathcal{F} be class of real functions and $\mathcal{H} = [\mathcal{F}_j]_{j=1}^k$ be a k -dimensional function class. If $\mathcal{A} : \mathbb{R}^k \rightarrow \mathbb{R}$ is a Lipschitz function with constant L and satisfies $\mathcal{A}(0) = 0$, then*

$$\hat{\mathcal{R}}_m(\mathcal{A} \circ \mathcal{H}) \leq 2kL\hat{\mathcal{R}}_m(\mathcal{F}).$$

Lemma 7 (Theorem 1 of [59]). *Let $\psi : \mathbb{R}^N \mapsto \mathbb{R}$ be a strictly convex differentiable function, and $D_\psi : \mathbb{R}^N \times \mathbb{R}^N \mapsto \mathbb{R}$ is the Bregman divergence induced by ψ . Let Y be an arbitrary random variable taking values in \mathbb{R}^N for which both $\mathbb{E}[Y]$ and $\mathbb{E}[\psi(Y)]$ are finite, we have*

$$\operatorname{argmin}_{\mathbf{s} \in \mathbb{R}^N} \mathbb{E}_Y[D_\psi(Y, \mathbf{s})] = \mathbb{E}[Y].$$